Interactive CLV3, CLE16, and CLE17 signaling mediates stem cell homeostasis in the Arabidopsis shoot apical meristem

Thai Q. Dao[1,2], Naama Weksler[1], Hannah M-H. Liu[1], Samuel Leiboff[2] and Jennifer C. Fletcher[1,*]

[1]Plant Gene Expression Center, United States Department of Agriculture-Agricultural Research Service, Albany, California, 94710 USA and University of California, Berkeley, California, 94720 USA

[2]Department of Botany and Plant Pathology, Oregon State University, Corvallis, Oregon, 97330 USA

[*]Corresponding author: Jennifer C. Fletcher

Plant Gene Expression Center, 800 Buchanan Street, Albany, CA 94710 USA

E-mail: jfletcher@berkeley.edu

Tel: +1 510 559 5917 Fax: +1 510 559 5678

The authors responsible for distribution of materials integral to the findings presented in this article in accordance with the policy described in the Instructions for Authors are: Thai Q. Dao (daoth@oregonstate.edu), and Jennifer C. Fletcher (jfletcher@berkeley.edu).

Abstract

The ability of plants to grow and form organs throughout their lifetime is dependent on their sustained stem cell activity. These stem cell populations are maintained by intricate networks of intercellular signaling pathways. In *Arabidopsis thaliana*, the small secreted peptide CLAVATA3 (CLV3) controls shoot apical meristem (SAM) maintenance by activating a signal

transduction pathway that modulates the expression of the homeodomain transcription factor WUSCHEL (WUS). Here, we demonstrate that two CLV3-related peptides, CLE16 and CLE17, restrict stem cell accumulation in the absence of CLV3. CLE16 and CLE17 contribute independently to SAM maintenance and organ production in *clv3* plants at all stages of development. We show that CLE16 and CLE17 signal through a subset of CLV3 receptors, the BARELY ANY MERISTEM (BAM) receptor kinases, and act upstream of WUS. Our study reveals that CLE16 and CLE17 function in a mechanism that partially compensates for CLV3 to maintain stem cell homeostasis and plant resiliency, and expands the potential targets for enhancing yield traits in crop species.

Introduction

In both animals and plants, pluripotent stem cell populations persist and continuously divide to supply building materials for growth and regeneration. Primary aboveground growth in plants is mediated by the shoot apical meristem (SAM), which is maintained by an intricate intercellular communication network (Aichinger et al., 2012, Heidstra and Sabatini, 2014, Steeves and Sussex, 1989). The most apical region of the SAM harbors the stem cell reservoir. Descendants of these cells that are pushed into the periphery undergo rapid divisions before differentiating to form leaf and flower primordia, the latter of which also harbor their own stem cell reservoir to produce floral organs before terminating in fruit formation. Stem cell identity is maintained by molecular factors originating from directly underlying cells, collectively called the organizing center (OC) (Barton, 2010; Gaillochet and Lohmann, 2015; Soyars et al., 2016). In *Arabidopsis thaliana*, the master regulator of stem cell identity in the SAM is WUSCHEL (WUS) (Laux et al., 1996). *WUS* is expressed in the OC, and encodes a homeodomain transcription factor that promotes stem cell identity and suppresses differentiation in the overlying cells (Mayer et al., 1998; Yadav et al., 2011). The WUS protein moves into the stem cell domain to directly activate the transcription of *CLAVATA3* (*CLV3*), which encodes a prepropeptide that is secreted to the extracellular space and processed into a small 12-13 amino acid peptide hormone (Fletcher et al., 1999; Ito et al., 2006; Ohyama et al. 2008; Ni et al., 2011; Rojo et al., 2002; Xu et al., 2013; Yadav et al., 2011). This mature peptide interacts with receptors in the underlying cell layers, where it limits stem cell accumulation by restricting the *WUS* expression domain to the OC

(Brand et al., 2000). CLV3-WUS thus forms a core negative feedback loop that maintains stem cell homeostasis in the SAM as well as in the transient floral meristem (Somssich et al., 2016; Dao and Fletcher, 2017). As a result, loss-of-function *clv3* mutants have enlarged shoot meristems that produce flowers with extra organs, whereas *CLV3* overexpression leads to premature SAM termination and growth arrest (Brand et al., 2000; Clark et al., 1996; Strabala et al., 2006).

Several complexes of leucine-rich repeat receptor-like kinases function to transduce the CLV3 signal. CLAVATA1 (CLV1) forms homodimers that localize to the cells directly below the *CLV3* expression domain and physically interact with CLV3 peptide (Clark et al., 1997; Ogawa et al., 2008). CLAVATA2 (CLV2) and its co-receptor CORYNE (CRN) form heterodimers throughout the SAM and transduce the CLV3 signal independently of CLV1, although it is unclear whether CLV2/CRN directly binds CLV3 (Müller et al., 2008; Bleckmann et al., 2010; Guo et al., 2010). Three BARELY ANY MERISTEM (BAM) receptors localize to the periphery of the SAM in a complementary manner to CLV1 (DeYoung et al., 2006; DeYoung et al., 2008; Nimchuk et al., 2015). BAM1 binds CLV3 *in vivo*, and *BAM1* and *BAM3* expression is excluded from the SAM interior by CLV1 activity (Nimchuk et al., 2017; Shinohara and Matsubayashi, 2015). While *bam1/2/3* triple mutants show a reduction in SAM size, *clv1 bam1/2/3* plants display a dramatic enhancement of stem cell accumulation beyond that of *clv3* plants. Thus, a dual activity model suggests that under normal conditions, the BAM receptors prevent CLV3-CLV1 signaling on the flanks of the SAM to maintain stem cell accumulation. However, when CLV1 is absent, *BAM* gene expression extends into the SAM center, which allows the receptors to partially compensate for the absence of CLV1 by interacting with CLV3 peptides (Nimchuk, 2017).

CLV3 is a member of a family of polypeptides called the CLAVATA3/EMBRYO SURROUNDING REGION-RELATED (CLE) peptides (Cock and McCormick, 2001). *CLE* genes are conserved throughout the land plant lineage, and their origination is concurrent with the evolution of three-dimensional growth in plants (Goad et al., 2016; Whitewoods et al., 2018). The Arabidopsis genome contains 32 *CLE* sequences encoding 27 distinct peptides (Jun et al., 2008). Only a handful of *CLE* genes have been functionally characterized, all of which are involved in diverse developmental processes (Wang et al., 2016). However, the majority of *cle*

single mutants have a wild-type phenotype, likely due to the high degree of redundancy typical of large gene families (Jun et al., 2010b). Indeed, evidence suggests that multiple CLE peptides may also function in the *Arabidopsis* SAM, as a previous study reported the promoter activity of several *CLE* genes in or around the shoot meristem (Jun et al., 2010b). A *dodeca-cle* mutant in which *CLV3* and 11 other *CLE* genes were knocked out using genome editing showed a more severe meristem phenotype than *clv3* plants, demonstrating that at least some of these 11 CLE peptides can partially compensate for CLV3 activity (Rodriguez-Leal et al., 2019). However, it is still unknown exactly which *CLE* genes are responsible for this compensation activity, nor the signaling pathway(s) through which they function.

Previously, we analyzed lines containing null alleles of *CLE16* and *CLE17*, which despite their promoter activity in the SAM displayed wild-type phenotypes under normal growth conditions (Gregory et al., 2018). In this study, we address the biological function of these CLE peptides by analyzing higher order *cle16*, *cle17* and *clv3* mutant combinations. Our work reveals that CLE16 and CLE17 partially compensate for CLV3 activity in stem cell maintenance beginning in embryogenesis and continuing throughout development, and that *CLV3*, *CLE16*, and *CLE17* together limit axillary branch number. Using peptide treatments, we demonstrate that CLE16 and CLE17 peptides are perceived by the BAM receptor kinases but not by CLV1 or CLV2. Finally, we show that, like CLV3, CLE16 and CLE17 signal in the same pathway as *WUS* to restrict shoot and floral stem cell accumulation. These results show that CLE16 and CLE17 are part of a molecular mechanism that compensates for CLV3 activity to maintain stem cell homeostasis by acting through a subset of CLV3 receptors at the shoot apex.

Results

CLE16 and *CLE17* expression in shoot meristems

In a previous comprehensive expression analysis, the *CLE16* and *CLE17* promoters were both shown to be active in the vegetative shoot apex (Jun et al., 2010b). To independently assess their expression dynamics, we performed mRNA *in situ* hybridization (ISH) to detect *CLE16* and *CLE17* transcripts in wild-type Col-0 vegetative meristems (VMs) and inflorescence meristems (IFMs). Neither *CLE16* nor *CLE17* transcripts were detectable in wild-type VMs (Fig. 1A, C).

Sense probes derived from *CLE16* and *CLE17* coding sequences were used as negative controls and showed no non-specific hybridization (Fig. S1A, C). In wild-type IFMs, *CLE16* and *CLE17* antisense probes also produced signals indistinguishable from those of the sense probes (Fig. 1I, L, Fig. S1E, H). Our results indicate that, although their promoters are active in shoot apex tissues, *CLE16* and *CLE17* transcripts are expressed at levels too low to be detected by ISH in wild-type shoot meristems.

Considering the possibility that CLE peptides act redundantly in the shoot apex, we used ISH to examine *CLE16* and *CLE17* expression in *clv3* and *clv3 cle16 cle17* SAMs. We observed a broad signal for *CLE16* transcripts in *clv3* VMs, with the strongest expression in the outer cell layers as well as in the organ primordia (Fig. 1B). In contrast, we were unable to detect *CLE17* transcripts in *clv3* vegetative shoot apices (Fig. 1D). In *clv3* IFMs, the *CLE16* antisense probe produced a signal in L1 cells that resembled that of the sense control, suggesting it might be an artifact (Fig. 1J, Fig. S1F). In contrast, the *CLE17* antisense probe produced a strong and specific signal in L1 cells (Fig. 1M, Fig. S1I). In *clv3 cle16 cle17* IFMs, both *CLE16* and *CLE17* were strongly up-regulated in the L1 cell layer compared to the negative controls (Fig. 1K, N, Fig. S1G, J). These results indicate that *CLE16* and *CLE17* transcription is dynamically repressed by CLV3 signaling during different phases of development. *CLE16* but not *CLE17* expression is down-regulated by CLV3 during the vegetative stage, whereas *CLE17* but not *CLE16* expression is down-regulated during the reproductive stage. Detection of both transcripts in *clv3 cle16 cle17* IFMs suggests that CLE16 and CLE17 signaling pathways potentially regulate themselves and/or each other.

Consistent with previous reports, *CLV3* and *WUS* transcripts were detected in the stem cells and organizing center, respectively, of Col-0 VMs and IFMs (Fig. 1E, G, O, R). The *CLV3* and *WUS* expression domains were likewise expanded in *clv3* and *clv3 cle16 cle17* VMs and IFMs (Fig. 1F, H, P, Q, S, T), indicating that CLE16 and CLE17 regulate stem cell homeostasis in a manner largely analogous to that of CLV3.

We also re-investigated *CLE16* and *CLE17* promoter activity in shoot apices of *pCLE16:*GUS-eGFP and *pCLE17:*GUS-eGFP reporter lines (Jun et al., 2010b) using confocal laser scanning microscopy (CLSM). Although neither reporter could be detected in wild-type or *clv3* VMs, we detected both *pCLE16:*eGFP and *pCLE17:*eGFP signal in the L1 layer of wild-type IFMs (Fig S1K, M), and *pCLE17:*eGFP but not *pCLE16:*eGFP signal in the L1 layer of *clv3* IFMs (Fig

S1L, N, O). However, signals for both reporters were discontinuous across the L1 layer. The disruption of *pCLE16:*eGFP and *pCLE17:*eGFP patterns across the L1 layer, as well as their incomplete overlap with the mRNA transcription patterns, suggest that these reporter constructs do not carry the full regulatory region. Nevertheless, both the ISH and GFP reporter experiments agree on *CLE16* and *CLE17* being expressed in the L1 layer of the IFM.

Finally, we examined *CLE16* and *CLE17* expression in a published gene expression map of Arabidopsis shoot apex domains (Tian *et al.* 2019). *CLE16* and *CLE17* showed the highest expression levels in the L1 layer and very low expression levels in the other regions of the SAM (Fig S2A, B), whereas *CLV3* transcripts accumulated specifically in the stem cells (Fig S2C). The absolute value of *CLV3* transcript levels as normalized RPKM was higher than that of both *CLE16* and *CLE17* (*CLV3*: 30.29, *CLE16*: 14.74, *CLE17*: 24.55, Fig S2A-C). Together, these data indicate that *CLE16* and *CLE17* are expressed at very low levels in the SAM, and their transcripts are concentrated in the L1 layer of the shoot apex.

CLE16 and *CLE17* buffer *CLV3* activity to restrict stem cell accumulation

CLE16 and *CLE17* encode mature CLE peptides that differ at a single amino acid from one another and at five amino acids relative to the CLV3 peptide (Fig. S3A). Unlike *clv3* mutants, *cle16* and *cle17* null mutants do not display shoot apical meristem phenotypes in Col-0 under normal growth conditions (Gregory et al., 2018). However, because the *CLE16* and *CLE17* promoters displayed overlapping expression patterns in the SAM, we hypothesized that the two genes function redundantly with each other and/or with *CLV3*. We tested this by generating *cle16-2 cle17-2*, *clv3-15 cle16-2*, *clv3-15 cle17-2*, and *clv3-15 cle16-2 cle17-2* plants carrying null alleles of *CLV3, CLE16* and/or *CLE17* (Table 1, Fig. S3B, C). We then compared SAM size across the embryonic, vegetative, and reproductive stages in these *cle16 cle17*, *clv3 cle16, clv3 cle17,* and *clv3 cle16 cle17* mutants and in wild-type Col-0 plants.

The CLV-WUS signaling pathway limits shoot apical meristem stem cell accumulation as early as the mature embryo stage (Schoof et al., 2000). We visualized the SAMs of mature embryos carrying the above allelic combinations using CLSM and found that the dimensions of *cle16 cle17* embryo SAMs were indistinguishable from those of the wild type (Fig. 2A, B, S). In

contrast, the diameter and height of *clv3* embryo SAMs was significantly greater than wild-type (Fig. 2A, C, S). Neither *clv3 cle16* nor *clv3 cle17* embryos displayed dramatic changes in SAM size relative to *clv3* embryos (Fig. 2C-E, S), although *clv3 cle16* embryos did show a small but significant increase in SAM diameter ($P = 0.03$). In contrast, *clv3 cle16 cle17* embryos formed SAMs that were significantly taller and broader than those of *clv3,* but not definitively larger than *clv3 cle16* or *clv3 cle17* embryos (Fig. 2C-F, S). These results show that *CLE16* and *CLE17* together restrict stem cell accumulation in the absence of *CLV3* beginning during embryogenesis. In addition, they suggest that either *CLE16* and *CLE17* act redundantly with one another at the embryonic stage, or their individual contributions are too subtle to measure at this stage under our experimental conditions.

At 7 days after germination (DAG), the vegetative meristems (VMs) of *cle16 cle17* plants remained indistinguishable from those of wild type plants, whereas *clv3* plants showed a dramatic VM size enhancement (Fig. 2G-I, T). *clv3 cle16* VMs were significantly larger in both height and diameter than *clv3* VMs (Fig. 2I, J, T), whereas *clv3 cle17* VMs were significantly wider but not taller than *clv3* VMs (Fig. 2I, K, T). *clv3 cle16 cle17* seedlings produced VMs that were significantly larger in all dimensions than those of *clv3* VMs, but were indistinguishable from *clv3 cle16* or *clv3 cle17* VMs (Fig. 2I-L, T). These results suggest that *CLE16* and *CLE17* independently restrict stem cell accumulation in *clv3* seedlings during vegetative development.

Analysis of IFM height and projected surface area revealed no differences in the dimensions of *cle16 cle17* IFMs compared to wild-type (Fig. 2M, N, U, Fig. S4A, B, G, H). In contrast, *clv3* plants formed fasciated IFMs that were significantly larger in both surface area and height than those of wild type IFMs (Fig. 2M, O, U, Fig. S4A, C, G, I). Although *clv3 cle16* plants did not exhibit increased IFM height or surface area compared to *clv3* plants, *clv3 cle17* plants showed significantly increased IFM surface area ($P < 10^{-4}$, Fig. 2O-Q, U, Fig. S4C-E, I-K), and *clv3 cle16 cle17* plants formed the largest IFMs on average (Fig. 2O-R, U, Fig. S4C-F, I-L). Both *CLE16* and *CLE17* therefore appeared to limit IFM activity in the absence of *CLV3* activity during reproductive development, with *CLE17* contributing more to stem cell restriction at this stage than *CLE16*.

Taken together, our results indicate that *CLE16* and *CLE17* each function to control stem cell accumulation in shoot meristems throughout development in the absence of endogenous *CLV3* activity. Furthermore, *clv3 cle17* plants form larger IFMs than *clv3 cle16* plants, indicating that *CLE17* plays a greater role than *CLE16* in restricting stem cell accumulation during reproductive development.

CLE16 and CLE17 buffer CLV3's ability to regulate lateral organ production

Because shoot meristematic activity directly influences the production of lateral organs such as leaves, axillary branches, and flowers, we also quantified these traits in Col-0, *cle16 cle17, clv3, clv3 cle16, clv3 cle17,* and *clv3 cle16 cle17* plants. Rosette leaf number was quantified at 21 DAG, once the plants completed vegetative development and entered the reproductive phase. Col-0 and *cle16 cle17* plants produced similar numbers of rosette leaves, whereas rosette leaf production was significantly enhanced in *clv3* plants (Fig. 3A). *clv3 cle16* plants produced a similar number of rosette leaves as *clv3* plants, but *clv3 cle17* plants generated significantly more leaves and *clv3 cle16 cle17* plants had the highest rate of rosette leaf production (Fig. 3A). Thus *CLV3* plays a role in limiting rosette leaf production during vegetative growth, most likely tied to its role in restricting shoot stem cell accumulation. *CLE17* performs this function in the absence of *CLV3,* and *CLE16* makes a minor contribution in the absence of the other two genes.

To measure axillary branching, plants were grown until 35 DAG, when axillary stems extending from the rosette were counted (Fig. 3B). Col-0 and *cle16 cle17* plants displayed a similar extent of axillary stem outgrowth, with an average of two per plant. In contrast, very little axillary stem outgrowth was observed in *clv3, clv3 cle16, clv3 cle17* and *clv3 cle16 cle17* plants (Fig. 3B). Thus, the number of visible axillary stems does not correlate with rosette leaf number, but rather their outgrowth appears to be inhibited in plants lacking CLV3 activity.

We next examined cauline leaf production and branch outgrowth from cauline leaf axils during reproductive development. At 35 DAG, Col-0 and *cle16 cle17* plants produced similar numbers of cauline leaves (Fig. 3C), whereas both *clv3* and *clv3 cle16* plants formed more than twice as many cauline leaves as wild-type plants. The cauline leaf production rate was significantly higher in *clv3 cle17* plants and the highest in *clv3 cle16 cle17* plants (Fig. 3C), mirroring the

phenotypes observed for the rosette leaves. With the exception of the triple mutant, the mean number of cauline axillary branches equaled the number of cauline leaves in all genotypes (Fig. 3D). In *clv3 cle16 cle17* plants, a few cauline leaves in each plant developed without a visible AM branch. As a result, despite having more cauline leaves, the mean number of visible AM buds in *clv3 cle16 cle17* plants was similar to that of *clv3 cle17* plants (Fig. 3C, D). Together, our data indicate that *CLV3*, *CLE16*, and *CLE17* together limit cauline axillary branch number by limiting the rate of cauline leaf production from the inflorescence meristem.

Finally, because the CLV-WUS signaling pathway is also active in the floral meristem (FM), we tested whether CLE16 and/or CLE17 could compensate for CLV3 activity during flower development. We used carpel number as a readout for floral meristem activity, because larger FMs produce more floral organs, and the carpels are the final whorl of organs to form as the FM undergoes termination. Whereas wild-type and *cle16 cle17* plants invariably made two carpels per flower, *clv3* plants made an average of one additional carpel (Fig. 3E-G, K). Mean carpel number was significantly enhanced in *clv3 cle16* and *clv3 cle17* flowers compared to *clv3* flowers, whereas *clv3 cle16 cle17* flowers generated significantly more carpels than either of the double mutants (Fig. 3G-K). We repeated this experiment with an independent set of null alleles (*clv3-10*, *cle16-3* and *cle17-3*, Fig. S3C, Table 1) and obtained similar results (Fig. S5). These data suggest that CLE16 and CLE17 also compensate for CLV3 signaling to restrict floral organ production.

Exogenous application of CLE16 and CLE17 peptide affects *clv3* meristems

In addition to our observation that CLV3 signaling represses *CLE16* transcript levels in vegetative meristems and *CLE17* transcript levels in reproductive meristems, we explored the possibility that CLV3 might interfere with the perception and/or transduction of CLE16 and CLE17 signals at the post-translational level as well. To test this scenario, we artificially induced CLE signaling in the SAM by germinating Arabidopsis seedlings on agar plates containing 30μM of synthetic CLV3, CLE16 or CLE17 peptides (Table 2). We used the unmodified 12-amino acid CLE sequences of the three peptides, as this portion of the CLV3 peptide is of comparable biological potency to the mature arabinosylated peptide at the concentration used

(Kim et al., 2017). We also used a peptide-free water treatment and a scrambled CLV3 (sCLE) amino acid sequence as negative controls.

We germinated Col-0, *cle16 cle17*, *clv3*, *clv3 cle16*, *clv3 cle17*, and *clv3 cle16 cle17* seeds on the peptide plates and measured vegetative SAM size in 7 DAG seedlings. Seedling SAM size among the genotypes was indistinguishable when grown on mock-treated or on sCLE plates (Fig. 4A-L), indicating that the scrambled peptide had no biological activity and that the experimental conditions had no effect on meristem function. In contrast, treatment with CLV3 peptide strongly reduced the SAM size of all genotypes, suggesting that the synthetic CLE peptides were effectively transported to the shoot apex, and that the unmodified CLV3 dodecapeptide was sufficient to limit *WUS* and stem cell activity in the SAM. In contrast, treatment with CLE16 or CLE17 peptides did not affect wild type or *cle16 cle17* seedling meristem size (Fig. 4A, B, G, H), indicating that neither CLE16 nor CLE17 synthetic peptides restrict SAM size in these genetic backgrounds. However, application of either CLE16 or CLE17 peptides significantly reduced SAM size in *clv3* plants compared to mock or sCLE treatments, albeit not to the same efficacy as CLV3 treatment (Fig. 4C, I). Similarly, CLE16 and CLE17 application significantly restricted stem cell accumulation in *clv3 cle16*, *clv3 cle17*, and *clv3 cle16 cle17* plants (Fig. 4D-F, J-L). These results suggest that endogenous CLV3 signaling prevents the biological activity of CLE16 and CLE17 peptides in the SAM.

To test the combined effect of CLE16 and CLE17 peptide treatment on meristem activity, we performed a peptide treatment of 7 DAG Col-0, *clv3*, and *clv3 cle16 cle17* plants using 15µM of CLV3, CLE16 or CLE17 synthetic peptides separately as well as a combination of 15µM CLE16 and 15µM CLE17 peptides (Fig. S6). Wild-type SAM height and diameter was restricted only by the application of CLV3 peptide (Fig. S6A), whereas *clv3* and *clv3 cle16 cle17* SAM size was restricted by all peptide treatments (Fig. S6B, C). In the latter two backgrounds CLV3 application had the strongest effect, while application of CLE16, CLE17 or CLE16+CLE17 peptides produced equivalent results (Fig. S6B, C). Notably, treatment with CLE16 and CLE17 together did not reduce SAM size more than treatment with either peptide alone, despite the total peptide concentration being higher. This observation suggests that the peptides reached an endogenous saturation level, and that CLE16 and CLE17 may act through the same signaling components that have rate-limiting capacity in these assays.

Receptor mutants confer resistance to distinct CLE peptides

The CLV3 signal at the shoot apex is transduced by a suite of receptor-like kinase complexes, including CLV1, BAM1 through BAM3, and potentially CLV2-CRN. Our peptide treatment experiment provides evidence that CLV3 blocks CLE16 and CLE17 signal transduction. Therefore, we tested the hypothesis that CLE16 and CLE17 could act through the same receptors as CLV3 by performing peptide treatment assays using *clv1-11*, *clv2-3*, and *bam1-4 bam2-4 bam3-2* loss-of-function receptor mutants as well as *clv1 clv3*, *clv2 clv3*, and *bam1/2/3 clv3* higher order mutant combinations.

Quantification of VM size in 5 DAG seedlings showed that treatment with synthetic CLV3 peptide significantly reduced both the height and diameter of *clv1* SAMs compared to mock treatment (Fig. 5A, I). That *clv1* mutants respond to CLV3 signaling is consistent with previous research showing that the BAM receptors compensate for the loss of CLV1 function (Nimchuk 2017). CLE16 and CLE17 treatment had no effect on *clv1* SAMs, most likely due to endogenous CLV3 activity (Fig. 5A, I). On the other hand, SAM size was effectively restricted when *clv1 clv3* plants were exposed to CLV3, CLE16, or CLE17 peptides (Fig. 5B, J), indicating that CLV1 is also dispensable for CLE16 and CLE17 signal transduction. *clv1 clv3* SAMs grown on CLE16 or CLE17 plates were not significantly different from those grown on CLV3 plates (Fig. 5B, J), suggesting that CLV1 receptor activity is responsible for most of the observed gap in biological efficacy between CLV3 and the CLE16 and CLE17 peptides.

Our assays revealed a complex role for the CLV2 receptor-like protein in CLE peptide perception. *clv2* SAM size was unaffected by CLV3, CLE16 or CLE17 peptide treatment (Fig. 5C, K). These data suggest that the CLE16 and CLE17 peptides can signal through CLV2, and additionally that either CLV2 is required to sense the synthetic CLV3 peptide or CLV2 controls stem cell accumulation independently of CLV3 signaling. However, *clv2 clv3* SAMs were clearly susceptible to the meristem-restricting effects of the CLV3, CLE16 and CLE17 peptides (Fig. 5D, L). CLV2 therefore appears to be only partially responsible for the full signal transduction of the CLV3, CLE16, CLE17 peptides in VMs. In addition, whereas *clv1 clv3* SAMs were very similar in size to *clv3* SAMs (Fig. 5B, H, J), *clv2 clv3* SAMs were significantly enlarged compared to *clv3* SAMs (Fig. 5D, H, L). This observation again indicates that at least

part of the meristem-restricting activity of the CLV2 pathway occurs independently of CLV3 signaling.

All genotypes examined exhibited a similar response to CLE16 and CLE17 peptide treatments except for *clv2 clv3* SAMs, which were more effectively restricted by CLE17 than by CLE16 application (Fig. 5D, L). Indeed, CLE17 was as effective as CLV3 in reducing SAM size in *clv2 clv3* plants (Fig. 5D, L). Thus, CLV2 might play a role in monitoring the stem cell response to the CLE16 and CLE17 peptides during vegetative development, either by increasing sensitivity to CLE16 or by dampening sensitivity to CLE17.

CLV3, CLE16 and CLE17 peptide treatments had distinct effects in the *bam* mutant background. *bam1/2/3* SAMs (Fig. 5E) were smaller than wild-type SAMs (Fig. 4A) when grown on mock-treated plates (Fig 5G, M), consistent with previous research suggesting a role for the BAM receptors in preventing excessive CLV3 signaling in the SAM periphery (Nimchuk et al. 2015). Like *clv1*, *bam1/2/3* SAM size was also restricted by exogenous CLV3 treatment, but was resistant to CLE16 and to CLE17 application (Fig. 5E, M). CLV3 treatment was also able to significantly reduce *bam1/2/3 clv3* SAM size (Fig. 5F, N). The BAM receptors are therefore not required for CLV3 signaling, a role that under normal circumstances is already performed by CLV1. In contrast, *bam1/2/3 clv3* SAMs were unaffected by the presence of CLE16 and CLE17 peptides (Fig. 5F, N). These results suggest that the BAM receptors are required to transmit the CLE16 and CLE17 signals. Finally, *clv1 bam1/2/3* plants were resistant to CLV3, CLE16, and CLE17 peptide application (Fig. 5O, P), indicating that these receptor kinases together play a crucial role in transducing multiple CLE signals at the shoot apex.

CLE16 and CLE17 function in the same pathway as WUS

While CLV3, CLE16 and CLE17 have differential interactions with downstream receptors, our current understanding of CLV1 and the BAM receptors suggests that these receptors all function upstream of the WUS transcription factor in the SAM. Therefore, we assessed whether *CLE16* and *CLE17* act in the same genetic pathway as *WUS* by crossing *cle16 cle17*, *clv3*, *clv3 cle16*, *clv3 cle17*, and *clv3 cle16 cle17* plants into the *wus-1* null mutant introgressed into the Col-0 background. Loss of WUS function leads to a SAM maintenance deficiency following initiation

(Laux et al., 1996). As a result, homozygous *wus* SAMs typically produce a few rosette leaves during vegetative growth and then prematurely arrest. Indeed, at 14 DAG, a wild-type Col-0 population segregating for the *wus-1* allele displayed a 3:1 ratio of wild-type to meristem-deficient phenotypes, with precocious termination of the primary shoot (Fig. 6A, Fig. S7A, Table 3). *cle16 cle17*, *clv3*, *clv3 cle16*, *clv3 cle17*, and *clv3 cle16 cle17* populations segregating for the *wus-1* allele showed the same proportion of plants with terminated primary shoots (Fig. 6A, Fig. S7B-F, Table 3), indicating that *wus* is epistatic to the *clv3*, *cle16* and *cle17* alleles. As a proxy for shoot meristem activity, we quantified the number of rosette leaves from these segregating populations, and observed that all individuals homozygous for *wus-1* produced the same limited number of rosette leaves, regardless of whether they carried the *clv3*, *cle16*, and/or *cle17* alleles (Fig. 6B). In contrast, plants that were not homozygous for *wus-1* produced many additional rosette leaves. Col-0 and *cle16 cle17* plants formed comparable numbers of rosette leaves, whereas plants homozygous for the *clv3* allele generated significantly more. Average rosette leaf number was similar between *clv3* and *clv3 cle16* plants, significantly higher in *clv3 cle17* plants, and higher still in *clv3 cle16 cle17* plants (Fig. 6B). Therefore, *WUS* acts downstream of *CLE16* and *CLE17* as well as of *CLV3*, and the function of CLE16 and CLE17 in primary SAM maintenance is dependent upon *WUS* activity.

Finally, we explored the possibility that, like *CLV3*, *CLE16* and *CLE17* expression is regulated by WUS activity. We queried a published WUS-regulated transcriptome dataset (Yadav et al., 2013), and found that neither *CLE16* nor *CLE17* was among the lists of transcripts directly or indirectly regulated by WUS. Although it is possible that *CLE16* and *CLE17* expression is too low to be detected in this experiment, we currently lack evidence that WUS regulates *CLE16* and *CLE17* transcription in the SAM.

Discussion

Plant stem cell reservoirs require molecular signals from neighboring cells to maintain homeostasis and continuously supply new cells for growth and organogenesis. In this study, we identified two CLE peptides, CLE16 and CLE17, that play important roles in buffering shoot stem cell homeostasis in the absence of CLV3 activity. CLE16 and CLE17 act in the same

genetic pathway as the BAM receptor kinases and the WUS transcription factor to control stem cell accumulation in the SAM.

Our previous study showed the *CLE16* and *CLE17* promoters are active in overlapping domains in vegetative and reproductive SAMs (Jun et al. 2010b). Because mature CLE peptides are cleaved from both ends of their precursor proteins (Ni et al., 2011, Xu et al., 2013), translational fusions of CLE coding sequences to fluorescent reporters currently do not exist. We therefore examined the *CLE16* and *CLE17* expression patterns in greater detail using ISH. Although we were unable to detect *CLE16* or *CLE17* mRNA transcripts in Col-0 VMs or IFMs, a published RNAseq-based gene expression database of Arabidopsis shoot apex domains shows that *CLE16* and *CLE17* transcripts accumulate in the outer L1 layer while being expressed at very low levels in the rest of the wild-type SAM (Tian et al. 2014). Consistently, *CLE16* mRNA expression was observed throughout the outer cell layers of *clv3* VMs and in the L1 cells of *clv3* IFMs (Fig. 1), while *CLE17* mRNA was not detected in *clv3* VMs but was present in the L1 cells of *clv3* IFMs. *CLE16* was more strongly up-regulated in the vegetative stage, and *CLE17* in the reproductive stage, in *clv3* IFMs (Fig. 1), consistent with *CLE17* contributing more than *CLE16* to restricting stem cell accumulation during reproductive development (Fig. 2, 3). Finally, both transcripts were detected in the L1 layer of *clv3 cle16 cle17* IFMs. We observed an imperfect overlap between the activities of the reporter lines and the transcript accumulation patterns (Fig S1), suggesting that cis-regulatory elements downstream of the transcription start site, which are absent from the reporter constructs, may be required for the dynamic pattern of *CLE16* and *CLE17* expression within the shoot apex (Fig 7A). Such cis-elements exist downstream of the *CLV3* stop site and are required for its dosage-dependent regulation by WUS (Perales et al., 2016). RT-qPCR assays did not detect up-regulation of *CLE16* or *CLE17* in *clv3* plants (Rodriguez-Leal et al., 2019). However, given the dramatic change in tissue size caused by the loss of *CLV3* function, and the higher sensitivity of ISH and reporter line analysis compared to other methods, we provide evidence that *CLE16* and *CLE17* expression is dynamically regulated by CLV3 activity. Due to the limitations of both ISH and RT-qPCR, methods such as FACS-based transcriptional profiling and/or single-cell RNA-seq will need to be employed to confirm the extent to which *CLE16* and *CLE17* are dynamically regulated within their respective expression domains.

Although CLE16 and CLE17 are dispensable for maintaining SAM function on their own (Gregory et al., 2018), our functional analysis reveals that in the absence of CLV3, both peptides play an important role in limiting shoot stem cell accumulation throughout the entire life cycle, with *CLE17* contributing more to restricting stem cell activity than *CLE16* in inflorescence and floral meristems. The major downstream output of the CLV3 signaling pathway is the negative regulation of the *WUS* expression domain (Mayer et al., 1998). *WUS* likewise acts downstream of *CLE16* and *CLE17* in the SAM, because in the absence of *WUS* even *clv3 cle16 cle17* plants are unable to sustain primary SAM growth (Fig. 6, Fig. S7). Such conditional cross-complementation among the CLV3 and CLE16/CLE17 signaling pathways may contribute to plant resiliency by buffering a critically important stem cell signaling network.

CLE16 and CLE17 signaling in the SAM is blocked at the post-translational level by endogenous CLV3 activity, because treatment with synthetic CLE16 or CLE17 peptides did not alter SAM activity in wild type or *cle16 cle17* plants yet effectively restricted stem cell accumulation in *clv3* mutants (Fig. 4). Although *CLE17* limits stem cell activity more effectively than *CLE16* during reproductive development, we see no evidence that the application of CLE17 peptide is more effective than that of CLE16 peptide in *clv3* seedlings (Fig. 4). Therefore, the biological response to endogenous CLE16 and CLE17 signaling may depend on a combination of dosage, expression patterns, and other dynamic downstream components that can act in a stage-specific manner.

CLV3 peptide can block CLE16 and CLE17 activity either by outcompeting them for binding to the same receptor kinases, or by preventing the biological activity of their cognate receptors in the SAM. Our peptide assays indicate that the BAM receptors, but not CLV1, transmit CLE16 and CLE17 signals in the SAM, consistent with CLE16 binding to the extracellular domain of the BAM1 receptor in vivo (Crook et al. 2020). These data are consistent with a CLE stem cell signaling model in which CLV1 is a specific receptor for CLV3, and CLV3-CLV1 signaling prevents BAM expression in the central SAM region. In the absence of CLV3 signal, the *BAM* gene expression domains extend into the SAM interior, enabling signaling via both CLV1 and the BAM receptors to affect stem cell activity (Fig. 7B). This model can explain our observation that synthetic CLV3 peptide is more effective than either CLE16 or CLE17 peptide at restricting stem cell accumulation in *clv3* plants, as CLV3 is able to interact with both CLV1 and the BAM proteins whereas CLE16 and CLE17 signal only through the BAM receptors.

Although peptide binding assays analyzing the specificity of the CLV1 and BAM receptors for the CLE16 and CLE17 peptides will be needed to further evaluate this scenario, it is tempting to speculate that the binding of CLE16 and CLE17 to the BAM receptors may be part of a mechanism that prevents CLV3 signaling on the meristem flanks. *cle16 cle17* SAMs are indistinguishable from wild type SAMs (Fig. 2-4), suggesting that CLE16 and CLE17 alone are not sufficient to perform this role. Yet in addition to CLV3, CLE16 and CLE17, other CLE peptides are perceived by the CLV1 and/or BAM receptors in the SAM, as both *clv3 cle16 cle17* plants and *dodeca-cle* plants display weaker meristem phenotypes than *clv1 bam1/2/3* plants that show severe defects in shoot architecture and flower development (Rodriguez-Leal et al., 2019). *CLE16* and *CLE17* are not among the genes mutated in the *dodeca-cle* background, suggesting some of these other CLE peptides may function redundantly with CLE16 and CLE17 to signal though the BAM receptors and regulate peripheral shoot stem cell activity.

Our work also sheds new light on the role of CLV2 in SAM stem cell signaling. CLV2 is implicated in various developmental processes *in planta*, and its function in the SAM requires interaction with other signaling components including CRN, CLV1, and the BAM receptors (Bleckmann et al., 2010; Zhu et al., 2010). Although CLV2 has not been shown to bind the arabinosylated 13-amino-acid (aa) CLV3 peptide, it is capable of binding the non-arabinosylated 12-aa CLV3 peptide form, as well as other CLE peptides with varying affinities (Guo et al., 2010; Shinohara and Matsubayashi, 2014). Our analysis shows that untreated *clv2 clv3* SAMs are larger than untreated *clv3* SAMs, and *clv2* SAM size is minimally affected whereas *clv2 clv3* SAMs are effectively restricted by application of 12-aa CLV3, CLE16 or CLE17 peptides (Fig. 5). We also observe that *clv2 clv3* plants respond differently to CLE16 and CLE17 peptide treatments than other genotypes. Whereas *clv1 clv3* and *bam1/2/3 clv3* plants respond similarly to CLE16 and CLE17 application, *clv2 clv3* plants are more strongly affected by CLE17 than CLE16 peptide. Thus, during vegetative development CLV2 may dampen the stem cell restricting effect of CLE17 or promote that of CLE16, perhaps by forming complexes with additional receptors and mediating their binding specificity. Our analysis therefore supports a dual function for CLV2: one that is independent of CLV3/CLE16/CLE17 signaling, and one that involves fine-tuning the meristem response to CLE16 and CLE17 in the absence of CLV3 activity.

Redundancy and compensation among CLE peptides and their cognate receptors appear to be a common feature throughout the land plant lineage. A dual CLE signaling system exists in the maize SAM, where the ZmFCP1 and ZmCLE7 peptide signals are transduced by a pair of receptor kinases (Je et al., 2016; 2017). In the tomato SAM, SlCLV3 is the dominant signal that restricts stem cell accumulation and SlCLE9 buffers the loss of SlCLV3 activity (Rodriguez-Leal et al., 2019). Observations in the moss *Physcomitrella patens* also suggest that multiple CLE peptides may control apical cell activity in leafy shoots via the partially redundant receptors PpCLV1a/b and PpRPK2 (Whitewoods et al., 2018). Plant stem cell activity underlies multiple yield traits such as branch number, fruit and seed number, and fruit size that are critically important for agricultural productivity (Li et al., 2021; Wang et al., 2021). It is therefore important to identify all of the genetic factors that control stem cell function, because manipulating any number of them could lead to agronomic improvements. By identifying two additional Arabidopsis *CLE* genes that signal to mediate stem cell activity, this work significantly expands our repertoire of candidate targets for crop yield enhancement.

Materials and methods

Plant materials and growth conditions

All *Arabidopsis thaliana* plants were in the Columbia-0 (Col-0) accession. The *clv3, cle16, cle17* and *bam* alleles were generated in Col-0, whereas the *clv1, clv2* and *wus* alleles were generated in Landsberg *erecta* (L-*er*) and introgressed 3-4 times into Col-0 prior to analysis. Plants were grown on a mixture of 1:1:1 mixture of perlite:vermiculite:top soil under long day conditions (16-hour light/8-hour dark, light intensity ~120 μmol/m^2/s) at 21˚C. Seeds were stratified at 4˚C for 5 days before exposure to light. Seedlings were watered daily with a 1:1500 dilution of Miracle-Gro 20-20-20 fertilizer prior to flowering and once a week with fertilizer thereafter. Homozygous plants were confirmed by PCR-based genotyping and restriction digestion (primers and restriction enzymes are listed in Table S1).

In situ hybridization

In situ hybridization was carried out as described in Jun et al. 2010a with a few modifications in the fixation process. Samples were fixed in a neutral buffered formalin solution (Sigma) overnight at 4˚C, washed in methanol at least three times for 15 min each, washed in ethanol twice for 10 min each, then transferred to a Leica TP1020 tissue processor for automated tissue infiltration into McCormick Paraplast X-tra. Samples were sectioned at 8 µm and transferred to microscope slides. After proteinase K digestion, samples were hybridized overnight at 55°C with sense and antisense RNA probes labeled with Digoxigenin (Roche) in a hybridization solution of 50% deionized formamide, 6X SSC, 3% SDS, 0.5 mg/mL tRNA. After washing with 2× SSC and 0.2× SSC, 0.2% SDS at 55-60°C, probes were detected by incubation with anti-Digoxigenin antibody linked to Alkaline Phosphatase (Roche) for 60 min to overnight. Visualization was carried out by incubation with nitro blue tetrazolium chloride – 5-bromo-4-chloro-3-indolyl-phosphate (NBT-BCIP, Roche) for 4-48 hours after washing. Tissue sections were imaged using a Leica DM4000 B light microscope (Leica Microsystems).

Peptide assays

For peptide treatment of seedlings, Murashige and Skoog (MS) growing medium, 0.7% agar, pH 5.7 was prepared and autoclaved. Before pouring, either water (mock) or a 3 mM solution of either synthetic scrambled peptide (sCLE), CLV3, CLE16, or CLE17 peptide (Genscript, purity ≥ 90%, no residue modification) in water was added to the MS medium to a final concentration of 30 µM. Arabidopsis seeds were sterilized in 70% ethanol followed by 10% bleach, 0.2% SDS and then plated on mock-treated or peptide-treated MS plates. Plants were grown under long day conditions and the shoot portions of the seedlings harvested five days after germination for confocal microscopy.

Confocal laser scanning microscopy

Propidium iodide (PI) staining of whole seedlings or organs was carried out as described in Truernit *et al.* 2008. To observe embryonic meristems, Arabidopsis seeds were imbibed in water overnight at 4˚C, and embryos were dissected from the seed coat for PI staining. Embryos and vegetative tissues were then cleared in methyl salicylate, whereas inflorescences were partially

embedded in 1% agarose in an upright position and submerged in water, before mounting on depression slides. Samples were visualized using a Leica TCS-SP8 spectral confocal laser scanning microscope (Leica Microsystems) with a 40X lens. The excitation/emission wavelengths were 488 nm/600-650 nm for PI, and 488 nm/500-530 nm for eGFP.

Phenotypic analysis

Shoot meristem measurements were performed as described (Monfared et al., 2013) using Fiji software. Parameters for each meristem were determined by defining three sets of coordinates: one for the apical point, and two for the notches where the meristematic zone ends and organ primordia begins. Meristem height and diameter were calculated as the height and base, respectively, of the resulting triangle. Z-stacks of inflorescence meristems were projected into 2-D images for surface area measurement, and reconstructed in Fiji's Volume Viewer for height measurement. Floral organ counting was performed as described (Fiume et al., 2010).

Acknowledgements

We thank Annis Richardson for technical consultation with CLSM, and Zachary Nimchuk and Sarah Hake for helpful comments on the manuscript. This work was supported by the US Department of Agriculture (CRIS grant 2030-21000-048-00D). This publication was made possible in part by award number 1337774 from the National Science Foundation, *MRI: Acquisition of Confocal and Two-Photon Excitation Microscope*. The authors wish to acknowledge the Confocal Microscopy Facility of the Center for Genome Research and Biocomputing at Oregon State University.

Author contributions

Designed experiments: TQD, JCF. Performed experiments: TQD, HL, NM. Analyzed data: TQD. Prepared figures: TQD. Designed project: TQD, JCF. Wrote and revised manuscript: TQD, JCF. Secured funding: SL, JCF.

References

Aichinger, E., Kornet, N., Friedrich, T., and Laux, T. (2012). Plant Stem Cell Niches. Annu. Rev. Plant Biol. **63**: 615–36.

Barton, M.K. (2010). Twenty years on : The inner workings of the shoot apical meristem, a developmental dynamo. Dev. Biol. **341**: 95–113.

Bleckmann, A., Weidtkamp-Peters, S., Seidel, C.A.M., and Simon, R. (2010). Stem cell signaling in Arabidopsis requires CRN to localize CLV2 to the plasma membrane. Plant Physiol. **152**: 166–76.

Clark, S.E., Jacobsen, S.E., Levin, J.Z., and Meyerowitz, E.M. (1996). The CLAVATA and SHOOT MERISTEMLESS loci competitively regulate meristem activity in Arabidopsis. Development **122**: 1567–1575.

Clark, S.E., Williams, R.W., and Meyerowitz, E.M. (1997). The CLAVATA1 gene encodes a putative receptor kinase that controls shoot and floral meristem size in Arabidopsis. Cell **89**: 575–585.

Cock, J.M. and McCormick, S. (2001). A large family of genes that share homology with CLAVATA3. Plant Physiol. **126**: 939–942.

Crook, A. D., Willoughby, A. C., Hazak, O., Okuda, S., VanDerMolen, K. R., Soyars, C. L., Cattaneo, P., Clark, N. M., Sozzani, R., Hothorn, M., Hardtke, C. S., Nimchuk, Z. L. (2020). BAM1/2 receptor kinase signaling drives CLE peptide-mediated formative cell divisions in Arabidopsis roots. Proc. Natl. Acad. Sci. U.S.A. **117** (51): 32750–32756.

Dao, T.Q. and Fletcher, J.C. (2017). CLE peptide-mediated signaling in shoot and vascular meristem development. Front. Biol. **12**: 406–420.

DeYoung, B.J. and Clark, S.E. (2008). BAM receptors regulate stem cell specification and organ development through complex interactions with CLAVATA signaling. Genetics **180**: 895–904.

DeYoung, B.J., Bickle, K.L., Schrage, K.J., Muskett, P., Patel, K., and Clark, S.E. (2006). The CLAVATA1-related BAM1, BAM2 and BAM3 receptor kinase-like proteins are required for meristem function in Arabidopsis. Plant J. **45**: 1–16.

Fiume, E., Monfared, M., Jun, J., and Fletcher, J.C. (2011). CLE polypeptide signaling gene expression in Arabidopsis embryos. Plant Signal. Behav. **6**: 443–444.

Fletcher, J.C. (2018). The CLV-WUS Stem Cell Signaling Pathway : A Roadmap to Crop Yield Optimization. Plants **7**: 87.

Fletcher, J.C., Brand, U., Running, M.P., Simon, R., and Meyerowitz, E.M. (1999). Signaling of cell fate decisions by CLAVATA3 in Arabidopsis shoot meristems. Science **283**: 1911–1914.

Forner, J., Pfeiffer, A., Langenecker, T., Manavella, P., and Lohmann, J.U. (2015). Germline-Transmitted Genome Editing in Arabidopsis thaliana Using TAL-Effector-Nucleases. PLoS One **10**: e0121056.

Gaillochet, C. and Lohmann, J.U. (2015). The never-ending story : from pluripotency to plant developmental plasticity. Development **142**: 2237–2249.

Goad, D.M., Zhu, C., and Kellogg, E.A. (2016). Comprehensive identification and clustering of CLV3/ESR-related (CLE) genes in plants finds groups with potentially shared function. New Phytol.: doi: 10.1111/nph.14348.

Gregory, E.F., Dao, T.Q., Alexander, M.A., Miller, M.J., and Fletcher, J.C. (2018). The signaling peptide-encoding genes CLE16, CLE17 and CLE27 are dispensable for Arabidopsis shoot apical meristem activity. PLoS One **13**: 1–16.

Guo, Y., Han, L., Hymes, M., Denver, R., and Clark, S.E. (2010). CLAVATA2 forms a distinct CLE-binding receptor complex regulating Arabidopsis stem cell specification. Plant J. **63**: 889–900.

Heidstra, R. and Sabatini, S. (2014). Plant and animal stem cells: similar yet different. Nat. Rev. Mol. Cell Biol. **15**: 301–12.

Ito, Y., Nakanomyo, I., Motose, H., Iwamoto, K., Sawa, S., Dohmae, N., and Fukuda, H. (2006). Dodeca-CLE peptides as suppressors of plant stem cell differentiation. Science. **313**: 842–845.

Je, B. Il et al. (2016). Signaling from maize organ primordia via FASCIATED EAR3 regulates stem cell proliferation and yield traits. Nat Genet **48**: 785–791.

Je, B. Il, Xu, F., Wu, Q., Liu, L., Meeley, R., and Jackson, D. (2017). The CLAVATA receptor FASCIATED EAR2 responds to different CLE peptides by signaling through different downstream effectors. Elife **7**: e35673.

Jun, J.H., Fiume, E., and Fletcher, J.C. (2008). The CLE family of plant polypeptide signaling molecules. Cell. Mol. Life Sci. **65**: 743–755.

Jun, J. H., Ha, C. M., Fletcher, J. C. (2010a). BLADE-ON-PETIOLE1 Coordinates Organ Determinacy and Axial Polarity in *Arabidopsis* by Directly Activating ASYMMETRIC LEAVES2. The Plant Cell **2010**, *22* (1), 62–76.

Jun, J., Fiume, E., Roeder, A.H.K., Meng, L., Sharma, V.K., Osmont, K.S., Baker, C., Ha, C.M., Meyerowitz, E.M., Feldman, L.J., and Fletcher, J.C. (2010b). Comprehensive analysis of CLE polypeptide signaling gene expression and overexpression activity in Arabidopsis. Plant Physiol. **154**: 1721–1736.

Kim, H., Wu, C., Yu, H., Sheen, J., Lee, H., Korea, S., Biology, I., and Hospital, M.G. (2017). Dual CLAVATA3 Peptides in Arabidopsis Shoot Stem Cell Signaling. J. Plant Biol. 60: 506–512.

Kimura, Y., Tasaka, M., Torii, K.U., and Uchida, N. (2018). ERECTA-family genes coordinate stem cell functions between the epidermal and internal layers of the shoot apical meristem. Development 145: dev156380.

Kondo, T., Sawa, S., Kinoshita, A., Mizuno, S., Kakimoto, T., Fukuda, H., and Sakagami, Y. (2006). A plant peptide encoded by CLV3 identified by in situ MALDI-TOF MS analysis. Science. **313**: 845–848.

Laux, T., Mayer, K.F.X., Berger, J., Jürgens, G., Genetik, L., and München, L. (1996). The WUSCHEL gene is required for shoot and floral meristem integrity in Arabidopsis. Development **122**: 87–96.

Li, S., Meng, S., Weng, J. and Wu, Q. (2021). Fine-tuning shoot meristem size to feed the world. Trends Plant Sci. doi.org/10.1016.j.plants.2021.10.004.

Mayer, K.F.X., Schoof, H., Haecker, A., Lenhard, M., Jürgens, G., Laux, T. (1998). Role of WUSCHEL in Regulating Stem Cell Fate in the Arabidopsis Shoot Meristem. Cell **95**: 805–815.

Monfared, M. M.; Fletcher, J. C. (2014) Genetic and Phenotypic Analysis of Shoot Apical and Floral Meristem Development. In Flower Development: Methods and Protocols; Riechmann, J. L., Wellmer, F., Eds.; Methods in Molecular Biology; Springer: New York, NY: 157–189.

Müller, R., Bleckmann, A., and Simon, R. (2008). The receptor kinase CORYNE of Arabidopsis transmits the stem cell-limiting signal CLAVATA3 independently of CLAVATA1. Plant Cell **20**: 934–46.

Ni, J. and Clark, S.E. (2006). Evidence for Functional Conservation, Sufficiency, and Proteolytic Processing of the CLAVATA3. Plant Physiol. **140**: 726–733.

Ni, J., Guo, Y., Jin, H., Hartsell, J., and Clark, S.E. (2011). Characterization of a CLE processing activity. Plant Mol. Biol. **75**: 67–75.

Nimchuk, Z.L. (2017). CLAVATA1 controls distinct signaling outputs that buffer shoot stem cell proliferation through a two-step transcriptional compensation loop. PLOS Genet. **13**: e1006681.

Nimchuk, Z.L., Zhou, Y., Tarr, P.T., Peterson, B.A., and Meyerowitz, E.M. (2015). Plant stem cell maintenance by transcriptional cross-regulation of related receptor kinases. Development **142**: 1043–9.

Ogawa, M., Shinohara, H., Sakagami, Y., and Matsubayashi, Y. (2008). Arabidopsis CLV3 Peptide Directly Binds CLV1 Ectodomain. Science **319**: 294–294.

Ohyama, K., Shinohara, H., Ogawa-Ohnishi, M., and Matsubayashi, Y. (2009). A glycopeptide regulating stem cell fate in Arabidopsis thaliana. Nat. Chem. Biol. **5**: 578–80.

Perales, M., Rodriguez, K., Snipes, S., Yadav, R.K., Diaz-Mendoza, M., and Reddy, G.V. (2016). Threshold-dependent transcriptional discrimination underlies stem cell homeostasis. Proc. Natl. Acad. Sci. 113: E6298–E6306.

Rodriguez-Leal, D. et al. (2019). Evolution of buffering in a genetic circuit controlling plant stem cell proliferation. Nat. Genet. **51**: 786–792.

Shinohara, H. and Matsubayashi, Y. (2015). Reevaluation of the CLV3-receptor interaction in the shoot apical meristem: dissection of the CLV3 signaling pathway from a direct ligand-binding point of view. Plant J. **82**: 328–336.

Somssich, M., Je, B. Il, Simon, R., and Jackson, D. (2016). CLAVATA-WUSCHEL signaling in the shoot meristem. Development **143**: 3238–3248.

Song, X., Xu, T., Ren, S., and Liu, C. (2013). Individual amino acid residues in CLV3 peptide contribute to its stability in vitro. Plant Signal. Behav. **8**: e25344.

Song, X., Yu, D., Xu, T., Ren, S., Guo, P., and Liu, C. (2012). Contributions of Individual Amino Acid Residues to the Endogenous CLV3 Function in Shoot Apical Meristem Maintenance in Arabidopsis. Mol. Plant **5**: 515–523.

Soyars, C.L., James, S.R., and Nimchuk, Z.L. (2016). Ready, aim, shoot: stem cell regulation of the shoot apical meristem. Curr. Opin. Plant Biol. **29**: 163–168.

Steeves, T.A. and Sussex, I.M. (1989). Patterns in Plant Development (Cambridge University Press: New York, NY).

Strabala, T.J., Donnell, P.J.O., Smit, A., Ampomah-Dwamena, C., Martin, E.J., Netzler, N., Nieuwenhuizen, N.J., Quinn, B.D., Foote, H.C.C., and Hudson, K.R. (2006). Gain-of-function phenotypes of many CLAVATA3/ESR genes, including four new family members, correlate with tandem variations in the conserved CLAVATA3/ESR domain. Plant Physiol. **140**: 1331–1344.

Su, Y.H., Zhou, C., Li, Y.J., Yu, Y., Tang, L.P., Zhang, W.J., Yao, W.J., Huang, R., Laux, T., and Zhang, X.S. (2020). Integration of pluripotency pathways regulates stem cell maintenance in the Arabidopsis shoot meristem. Proc. Natl. Acad. Sci.: doi: 10.1073/pnas.2015248117.

Tian, C.; Zhang, X.; He, J.; Yu, H.; Wang, Y.; Shi, B.; Han, Y.; Wang, G.; Feng, X.; Zhang, C.; Wang, J.; Qi, J.; Yu, R.; Jiao, Y. (2014) An Organ Boundary-Enriched Gene Regulatory Network Uncovers Regulatory Hierarchies Underlying Axillary Meristem Initiation. Mol Syst Biol, **10** (10), 1–2.

Tian, C.; Wang, Y.; Yu, H.; He, J.; Wang, J.; Shi, B.; Du, Q.; Provart, N. J.; Meyerowitz, E. M.; Jiao, Y. (2019) A Gene Expression Map of Shoot Domains Reveals Regulatory Mechanisms. Nat Commun, **10** (1), 141.

Truernit, E., Bauby, H., Dubreucq, B., Grandjean, O., Runions, J., Barthélémy, J., Palauqui, J.-C. (2008). High-Resolution Whole-Mount Imaging of Three-Dimensional Tissue Organization and Gene Expression Enables the Study of Phloem Development and Structure in *Arabidopsis*. The Plant Cell, *20* (6), 1494–1503.

Wang, C., Yang, X. and Li, G. (2021). Molecular insights into inflorescence meristem specification for yield potential in cereal crops. Int. J. Mol. Sci. **22**: 3508.

Wang, G., Zhang, G., and Wu, M. (2016). CLE Peptide Signaling and Crosstalk with Phytohormones and Environmental Stimuli. Front. Plant Sci. **6**: 1211.

Whitewoods, C.D. et al. (2018). CLAVATA Was a Genetic Novelty for the Morphological Innovation of 3D Growth in Land Plants. Curr. Biol. **28**: 1–12.

Xu, T.-T., Song, X.-F., Ren, S.-C., and Liu, C.-M. (2013). The sequence flanking the N-terminus of the CLV3 peptide is critical for its cleavage and activity in stem cell regulation in Arabidopsis. BMC Plant Biol. **13**: 225.

Yadav, R.K., Perales, M., Girke, T., and Jo, H. (2011). WUSCHEL protein movement mediates stem cell homeostasis in the Arabidopsis shoot apex. Genes Dev. **25**: 2025–2030.

Yadav, R. K.; Perales, M.; Gruel, J.; Ohno, C.; Heisler, M.; Girke, T.; Jönsson, H.; Reddy, G. V. (2013) Plant Stem Cell Maintenance Involves Direct Transcriptional Repression of Differentiation Program. Mol Syst Biol, **9**, 654.

Zhu, Y., Wang, Y., Li, R., Song, X., Wang, Q., Huang, S., Jin, J.B., Liu, C.M., and Lin, J. (2010). Analysis of interactions among the CLAVATA3 receptors reveals a direct interaction between CLAVATA2 and CORYNE in Arabidopsis. Plant J. **61**: 223–233.

Figures and Tables

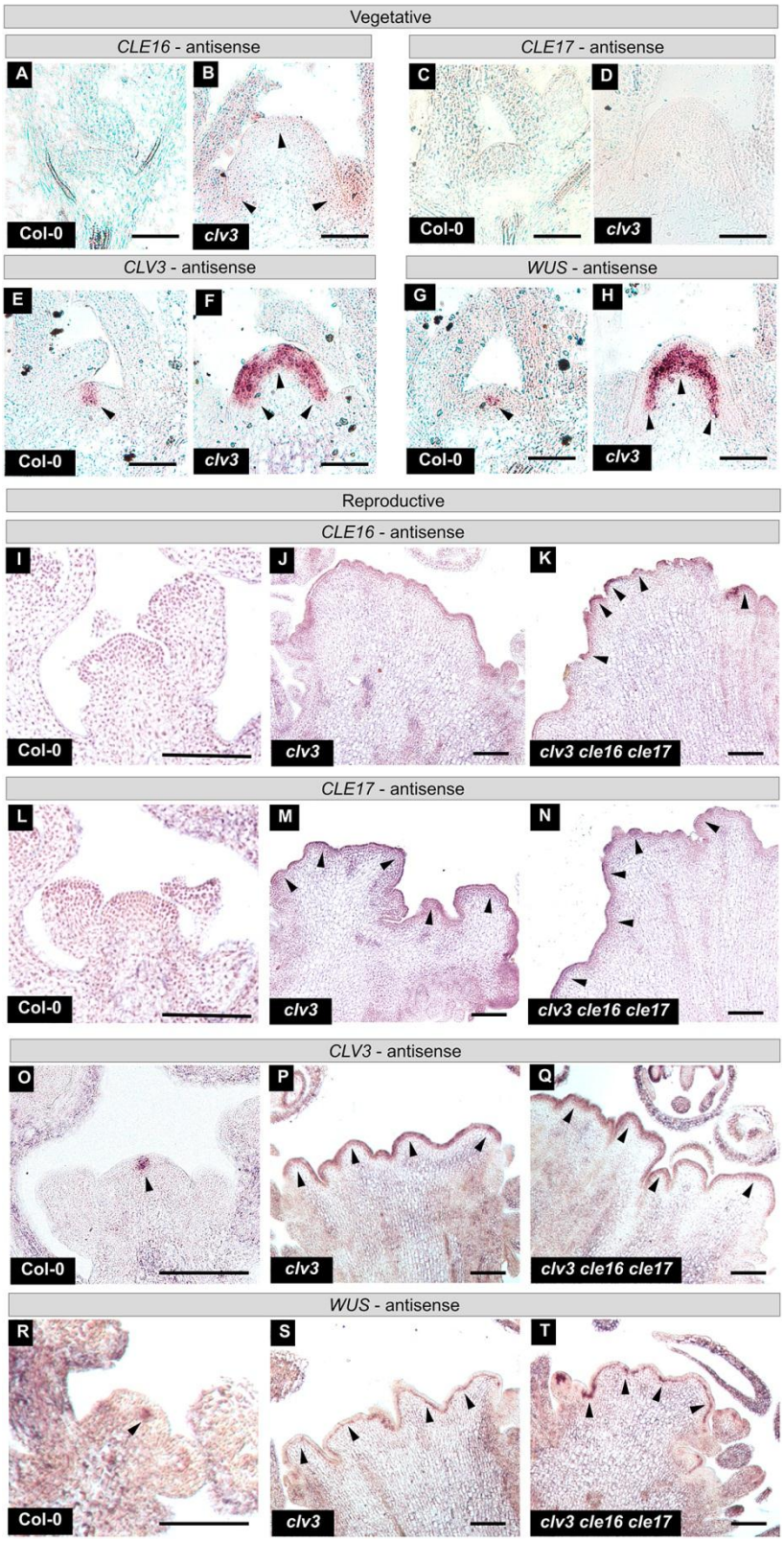

Fig. 1. mRNA expression patterns of *CLE16, CLE17, CLV3* and *WUS* in shoot meristems. A-H, mRNA *in situ* hybridization of *CLE16* (A, B), *CLE17* (C, D), *CLV3* (E, F), and *WUS* (G, H) antisense probes to wild-type Col-0 (A, C, E, G) and *clv3-15* (B, D, F, H) 7 DAG vegetative SAMs. I-T, mRNA *in situ* hybridization of *CLE16* (I-K), *CLE17* (L-N), *CLV3* (O-Q), and *WUS* (R-T) antisense probes to Col-0 (I, L, O, R), *clv3-15* (J, M, P, S) and *clv3 cle16 cle17* (K, N, Q, T) IFMs. Arrowheads highlight antisense probe accumulation. Scale bars: 50 µm in A-H, 100 µm in I-T.

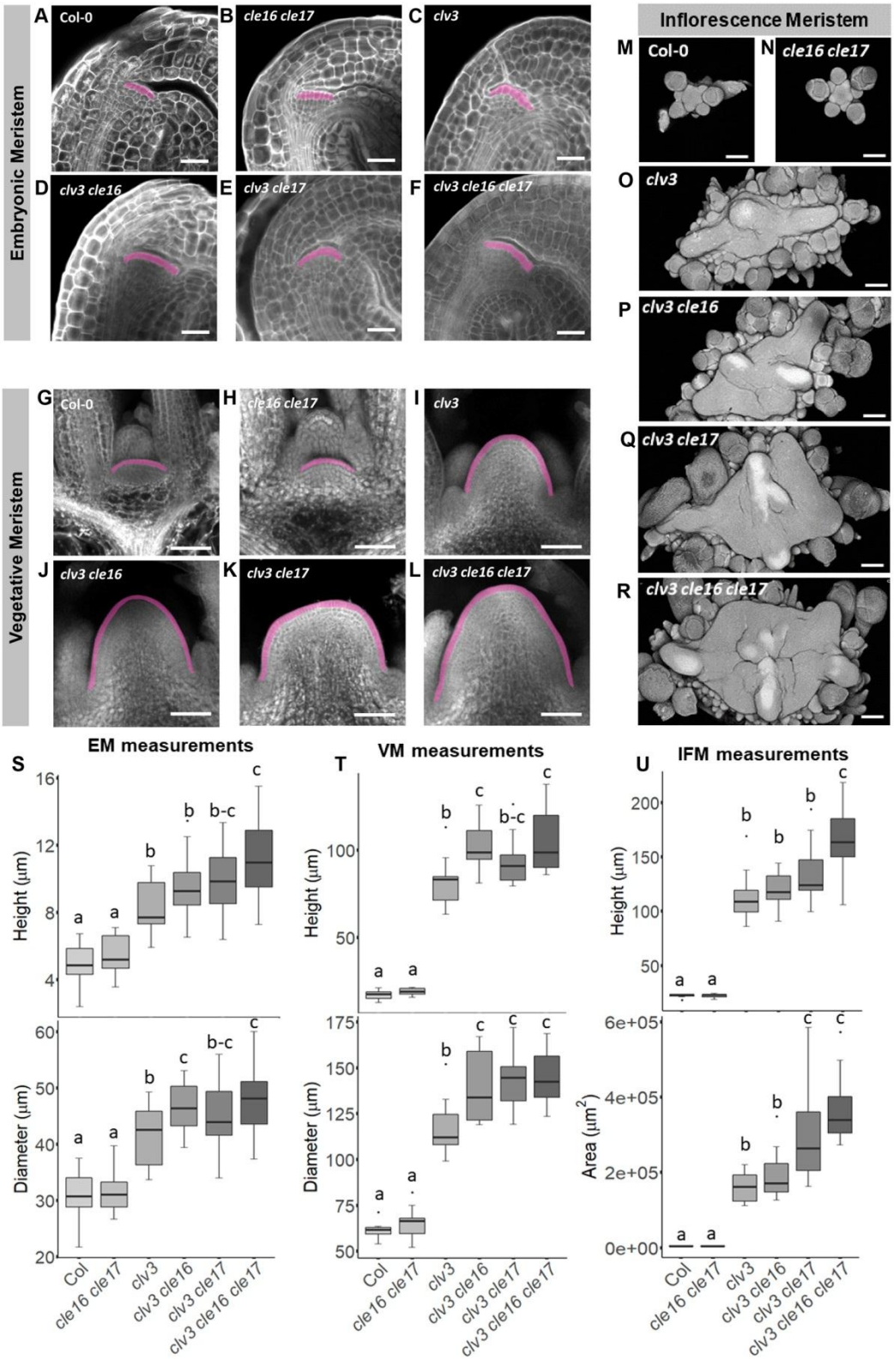

Fig. 2. *CLE16* and *CLE17* restrict stem cell accumulation in the SAM in the absence of *CLV3* activity. A-R, Confocal micrographs of Arabidopsis SAMs at the embryonic (A-F), vegetative (G-L), and reproductive stage (M-R) from wild-type (A, G, M), *cle16 cle17* (B, H, N), *clv3* (C, I, O), *clv3 cle16* (D, J, P), *clv3 cle17* (E, K, Q), and *clv3 cle16 cle17* (F, L, R) plants. Cells in the L1 layer are colored pink. S-U, Meristem size measurements at the embryonic (S), vegetative (T), and reproductive stage (U) from wild-type, *cle16 cle17*, *clv3*, *clv3 cle16*, *clv3 cle17*, and *clv3 cle16 cle17* plants. (S) n = 16-22, (T) n = 11-15, (U) n = 8-16. Statistical analysis was performed using one-way ANOVA and Tukey test; letters represent different significance groups at $P < 0.05$. Scale bars: 25 µm in (A-F), 50 µm in (G-L), 100 µm in (M-R).

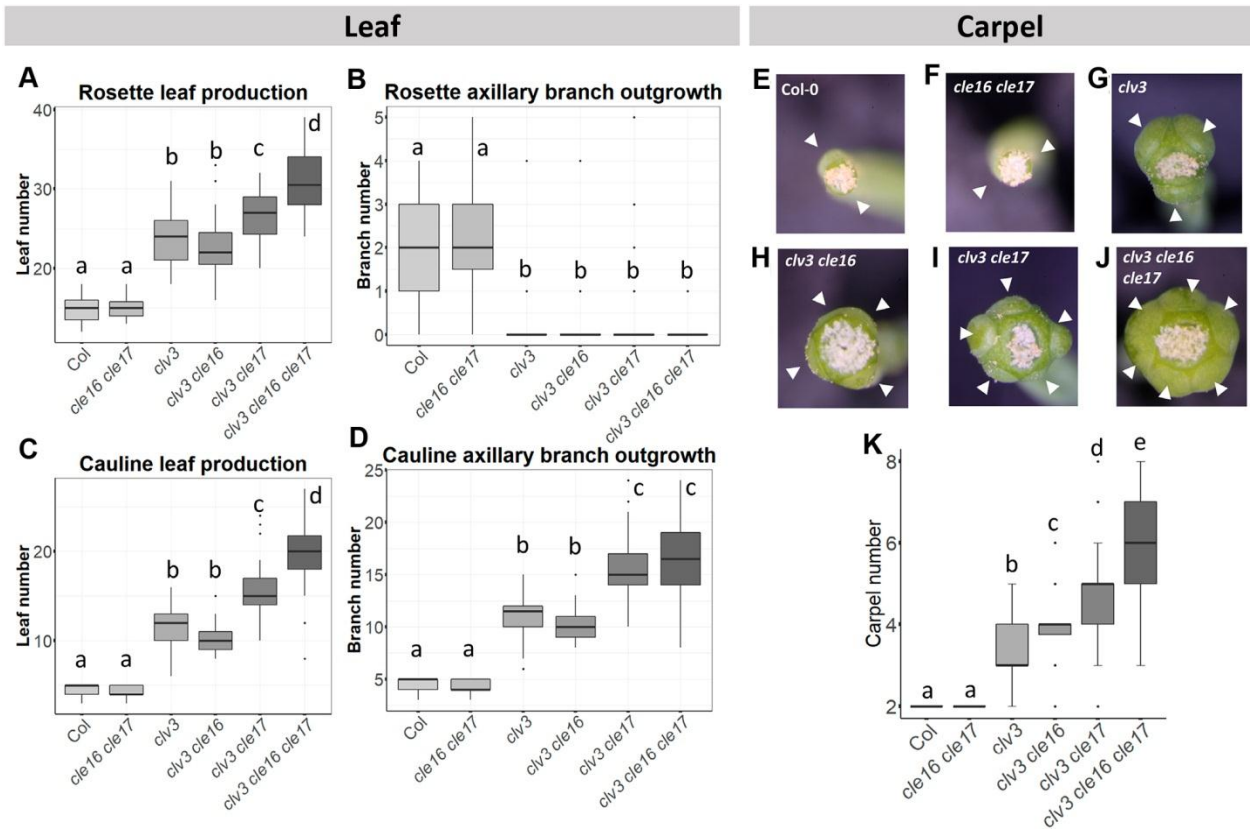

Fig. 3. *CLE16* and *CLE17* control lateral organ production in the absence of *CLV3* activity. A-B, Rosette leaf and axillary branch production during vegetative development, measured as (A) average rosette leaf number (n = 22-36), and (B) average outgrowing axillary branch number (n = 12-26) in wild-type, *cle16 cle17*, *clv3*, *clv3 cle16*, *clv3 cle17* and *clv3 cle16 cle17* plants. C-D, Cauline leaf and axillary branch production measured as (C) average cauline leaf number (n = 12-26), and (D) average outgrowing axillary branch number (n = 12-26). E-J, Top-down view of wild-type (E), *cle16 cle17* (F), *clv3* (G), *clv3 cle16* (H), *clv3 cle17* (I) and *clv3 cle16 cle17* (J) carpels. K, Mean carpel number per flower (n = 100). White arrowheads denote individual carpels. Statistical analysis was performed using one-way ANOVA and Tukey test; letters represent different significance groups at $P < 0.05$.

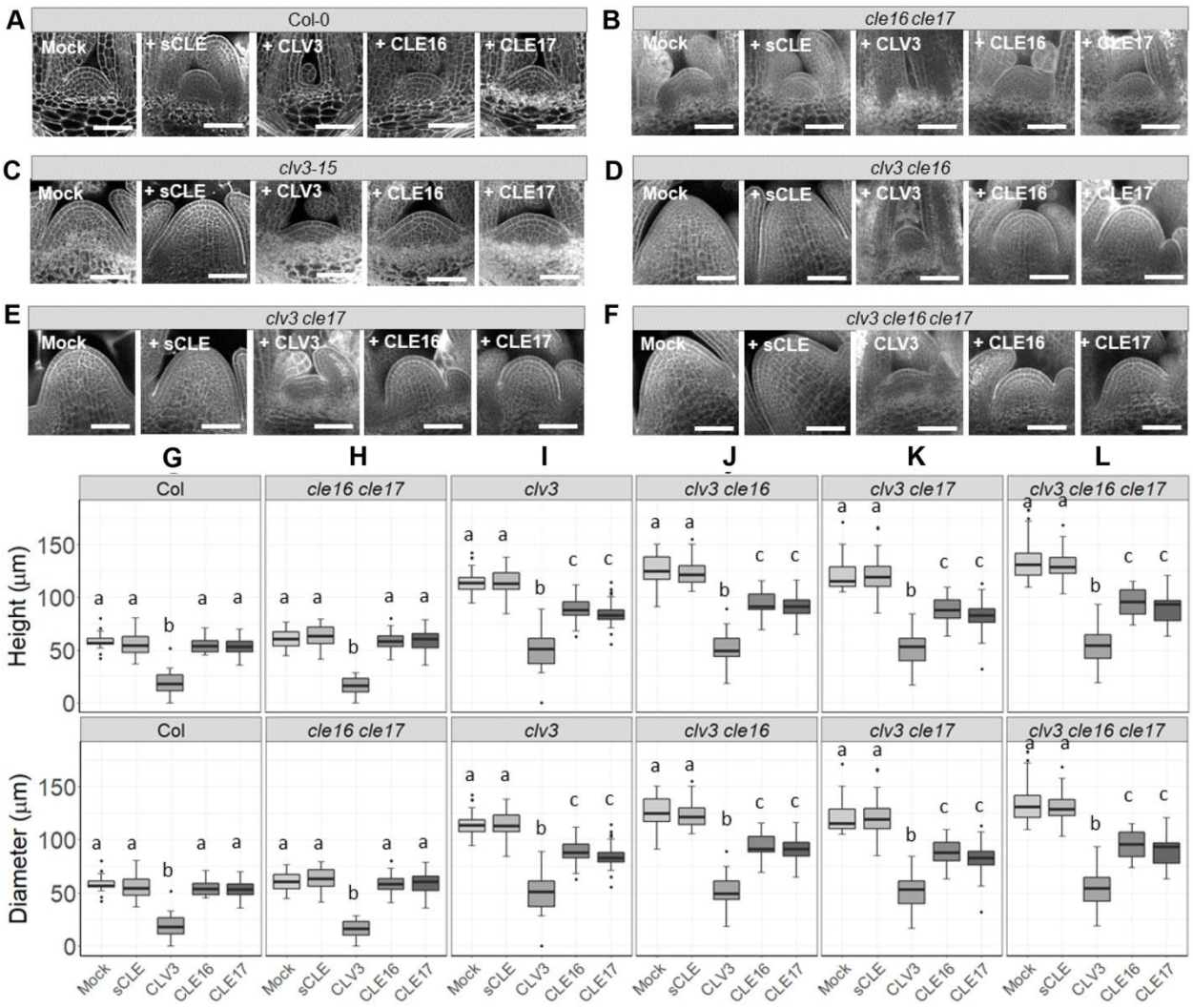

Fig. 4. CLE16 and CLE17 synthetic peptide treatments affect stem cell accumulation in the SAM in the absence of CLV3 activity. Confocal micrographs (A-F) and vegetative meristem size measurements (G-L) of 7 DAG wild-type (A, G), *cle16 cle17* (B, H), *clv3* (C, I), *clv3 cle16* (D, J), *clv3 cle17* (E, K), and *clv3 cle16 cle17* (F, L) plants grown without (mock) or with 30 µM of synthetic sCLE, CLV3, CLE16, or CLE17 peptide (n = 17-36). Statistical analysis was performed using one-way ANOVA and Tukey test; letters represent different significance groups at $P < 0.05$. Scale bars: 50 µm.

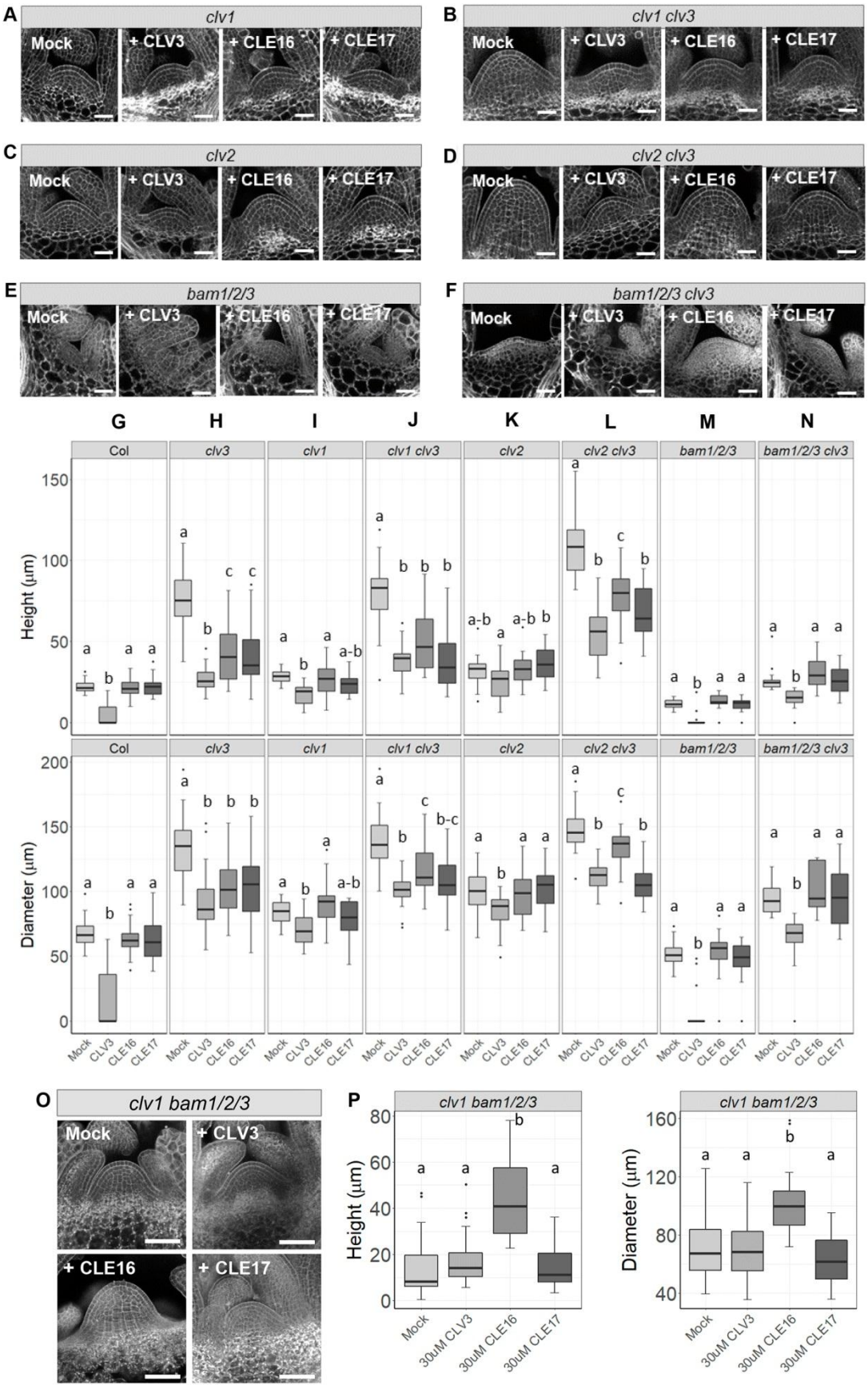

Fig. 5. Receptor kinase genes respond differentially to CLE16, CLE17 and CLV3 synthetic peptide treatments. Confocal micrographs (A-F) and vegetative meristem size measurements (G-N) of 5 DAG wild-type (G), *clv3* (H), *clv1* (A, I), *clv1 clv3* (B, J), *clv2* (C, K), *clv2 clv3* (D, L), *bam1 bam2 bam3* (E, M), *bam1 bam2 bam3 clv3* (F, N) plants grown without (mock) or with 30 µM synthetic CLV3, CLE16, or CLE17 peptide (n = 14-29). Confocal micrographs (O) and vegetative meristem size measurements (P) of 7 DAG *clv1 bam1 bam2 bam3* plants grown without or with 30 µM synthetic CLV3, CLE16, or CLE17 peptide (n = 16-45). Statistical analysis was performed using one-way ANOVA and Tukey test; letters represent different significance groups at $P < 0.05$. Scale bars: 25 µm for A-F, and 50 µm for O.

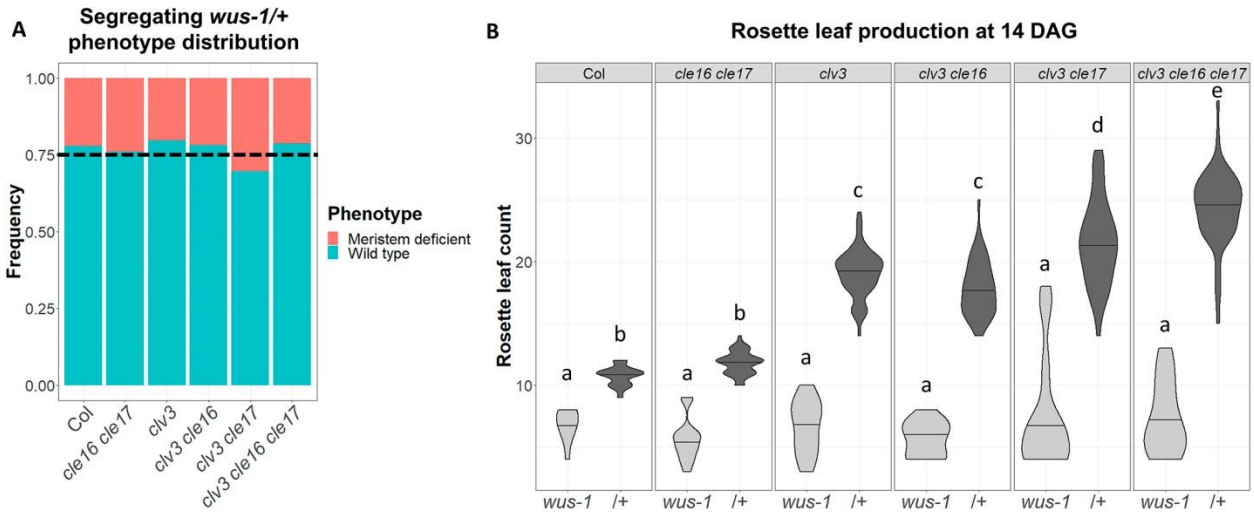

Fig. 6. *CLE16* and *CLE17* signaling acts upstream of *WUS*. Distribution of meristem-deficient phenotype (A) and average rosette leaf number (B) in wild-type, *cle16 cle17*, *clv3*, *clv3 cle16*, *clv3 cle17*, and *clv3 cle16 cle17* populations segregating for the *wus-1* allele (n = 50-74). Dashed line in (A) represents the expected 1:3 ratio of meristem deficient to wild-type phenotypes. Statistical analysis was performed using one-way ANOVA and Tukey test; letters represent different significance groups at $P < 0.05$.

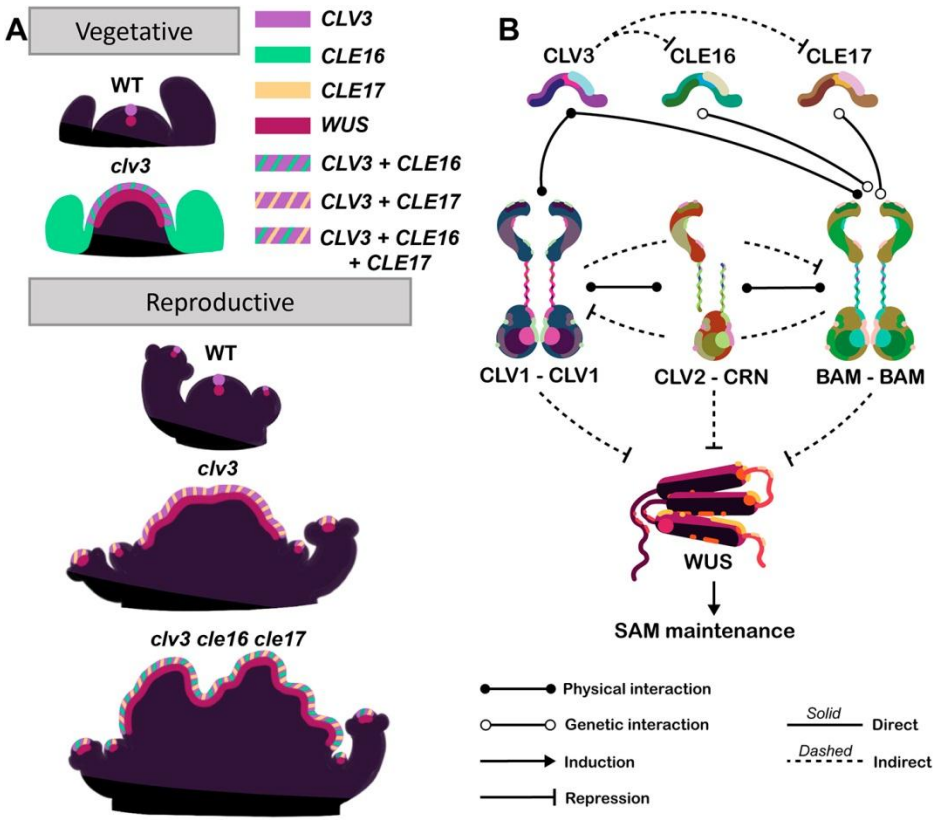

Fig. 7. Model of CLV3, CLE16, and CLE17 activity in the SAM. A, Schematic of *CLV3*, *CLE16*, *CLE17*, and *WUS* expression patterns in wild-type, *clv3*, and *clv3 cle16 cle17* SAMs at the vegetative and reproductive stage. B, Schematic of CLV3, CLE16 and CLE17 peptide perception and signaling in the SAM. CLV3 can physically interact with the CLV1 and BAM receptor kinases. CLV3 signaling through CLV1 excludes *BAM* gene expression from the central region of the SAM, whereas BAM receptor kinase activity blocks CLV3-CLV1 signaling from the peripheral region. The CLV2-CRN complex can interact with CLV1 and the BAM proteins to fine-tune their activity. CLE16 and CLE17 can signal through the BAM receptors, but are blocked by CLV3 activity under normal conditions. CLE signaling through the various receptors restricts the *WUS* expression domain to regulate stem cell homeostasis in the SAM.

Table 1. List of CLE alleles used in this study

Gene	Allele	Type of Mutation	Effect on protein	Source
CLV3 (AT2G27250)	*clv3-10*	Deletion of 5 bp at +550	Deletion and frameshift in the CLE domain starting at aa 76	Forner *et al.* 2015
	clv3-15	Deletion of 78 bp and insertion of 8 bp at +547	Deletion of half of the CLE domain starting at aa 75	Forner *et al.* 2015
CLE16 (AT2G01505)	*cle16-2*	Insertion of C at +59	Premature stop codon at aa 45	Gregory *et al.* 2018
	cle16-3	Deletion of G at +59	Frameshift at aa 20	Gregory *et al.* 2018
CLE17 (AT1G70895)	*cle17-2*	Insertion of A at +220	Premature stop codon at aa 80	Gregory *et al.* 2018
	cle17-3	Insertion of T at +220	Premature stop codon at aa 80	Gregory *et al.* 2018

Table 2. Synthetic peptide sequences used in this study

Peptide	Sequences
sCLE	PPTRGLSHHPVD
CLV3	RTVPSGPDPLHH
CLE16	RLVHTGPNPLHN
CLE17	RVVHTGPNPLHN

Table 3. Phenotype distribution of populations segregating for the *wus-1* allele

Genetic background	*wuschel* phenotype	WT phenotype	Total	Expected	X-square	p
Col	15	53	68	17	0.314	0.575
cle16 cle17	12	38	50	13	0.104	0.747
clv3	15	59	74	19	1.133	0.287
clv3 cle16	14	50	64	16	0.333	0.564
clv3 cle17	20	46	66	17	0.713	0.398
clv3 cle16 cle17	15	55	70	18	0.673	0.412

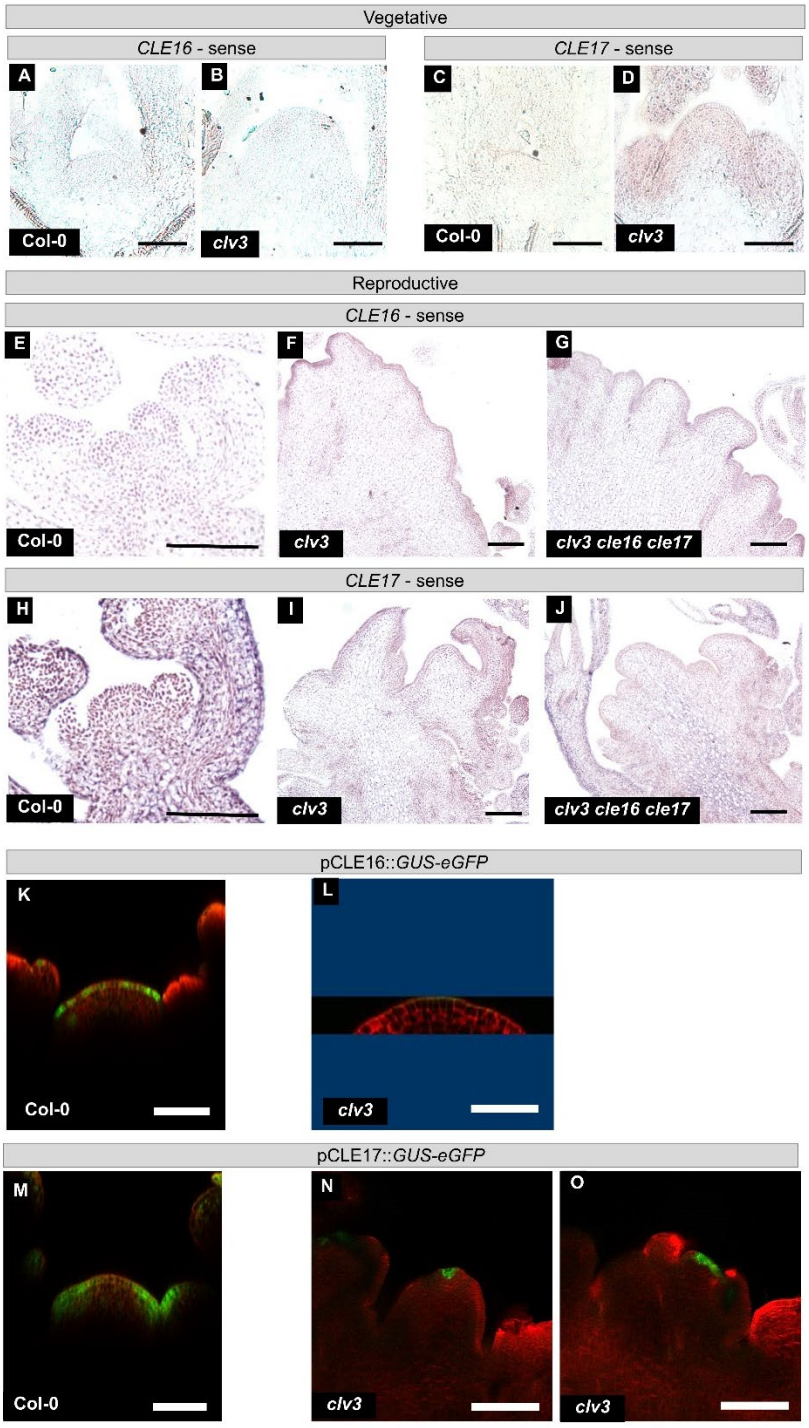

Fig. S1. CLE16 and CLE17 expression patterns in vegetative and reproductive shoot meristems, related to figure 1. A-D, Sense probe controls for mRNA *in situ* hybridization of *CLE16* (A, B) and *CLE17* (C, D) to 7 DAG vegetative SAMs of wild-type (A, C) and *clv3-15* (B, D) plants. E-J, Sense probe controls for mRNA *in situ* hybridization of *CLE16* (E-G) and *CLE17* (H-J) to IFMs of Col-0 (E, H), *clv3-15* (F, I) and *clv3 cle16 cle17* (G, J) plants. K-O, Confocal micrographs showing expression of pCLE16::GUS-eGFP (K, L) and pCLE17:GUS::eGFP (M-O) reporters in wild-type (K, M) and *clv3* (L, N, O) IFMs. Images in K, L, Mare reconstructed longitudinal sections from z-stacks. Images in N, O are single plane captures. Scale bars: 50 μm in A-D, 100 μm in E-O.

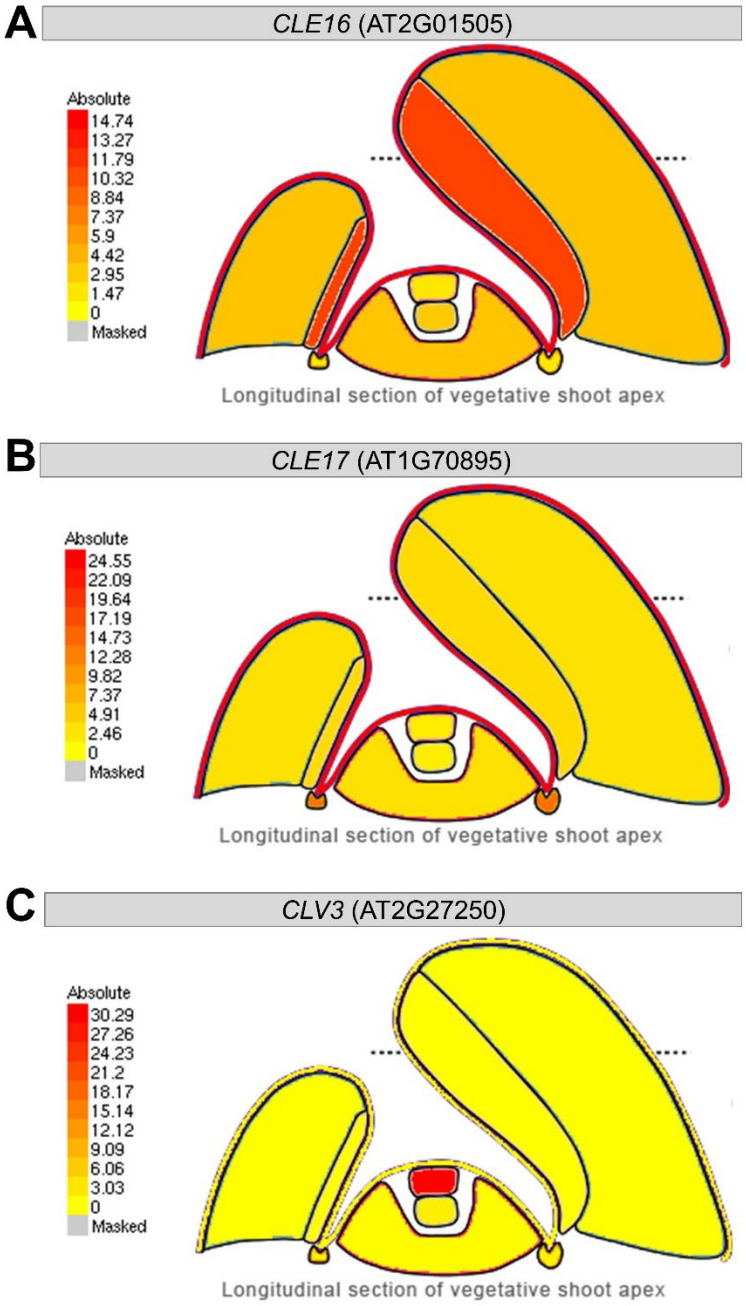

Fig. S2. eFP browser view of *CLE16, CLE17, CLV3,* and *ATML1* expression levels in Arabidopsis vegetative shoot meristems and leaf primordia, related to figure 1. *CLE16* (A), *CLE17* (B), and *CLV3* (C) normalized to RPKM units. An average of triplicates is shown. RNA-seq source data from Tian et al. (2014) and Tian et al. (2019).

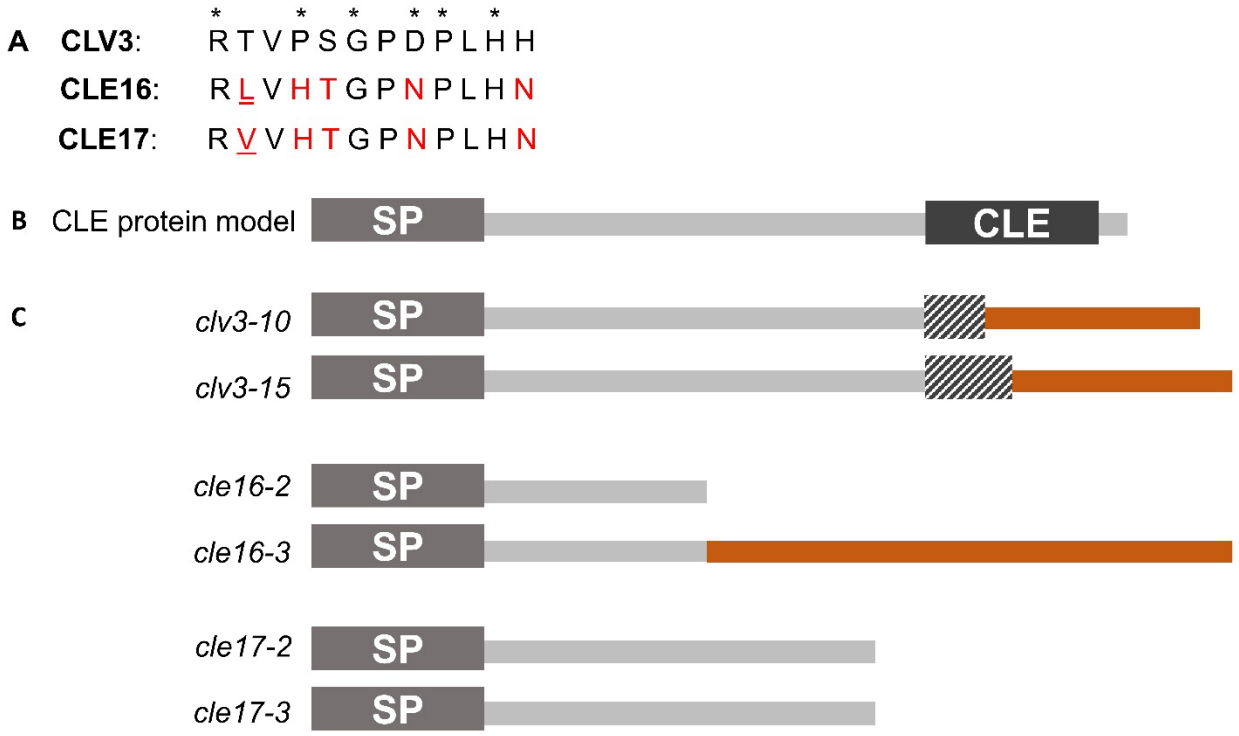

Fig. S3. CLE peptides and alleles used in this study. A, Alignment of the CLV3, CLE16, and CLE17 CLE domains. Asterisks denote amino acids in CLV3 that are important for receptor binding. Black text denotes amino acids that are conserved between all three proteins. B, Schematic of a generic CLE protein with an amino terminal signal peptide (SP), followed by a variable region and a 13 amino acid CLE domain. C, Schematics of mutant CLE pre-pro-peptides generated by the alleles used in this study. The *clv3-10* allele leads to a deletion and frameshift in the region encoding the CLV3 domain. The *clv3-15* allele leads to deletion of half of the CLV3 domain and its replacement with 36 random amino acids. The *cle16-3* allele leads to a frameshift upstream of the CLE domain. The *cle16-2*, *cle17-2* and *cle17-3* alleles each result in a premature stop codon upstream of the CLE domain. Hatched boxes denote deletions, and red lines denote random amino acid sequences induced by frameshifts in the mutant alleles.

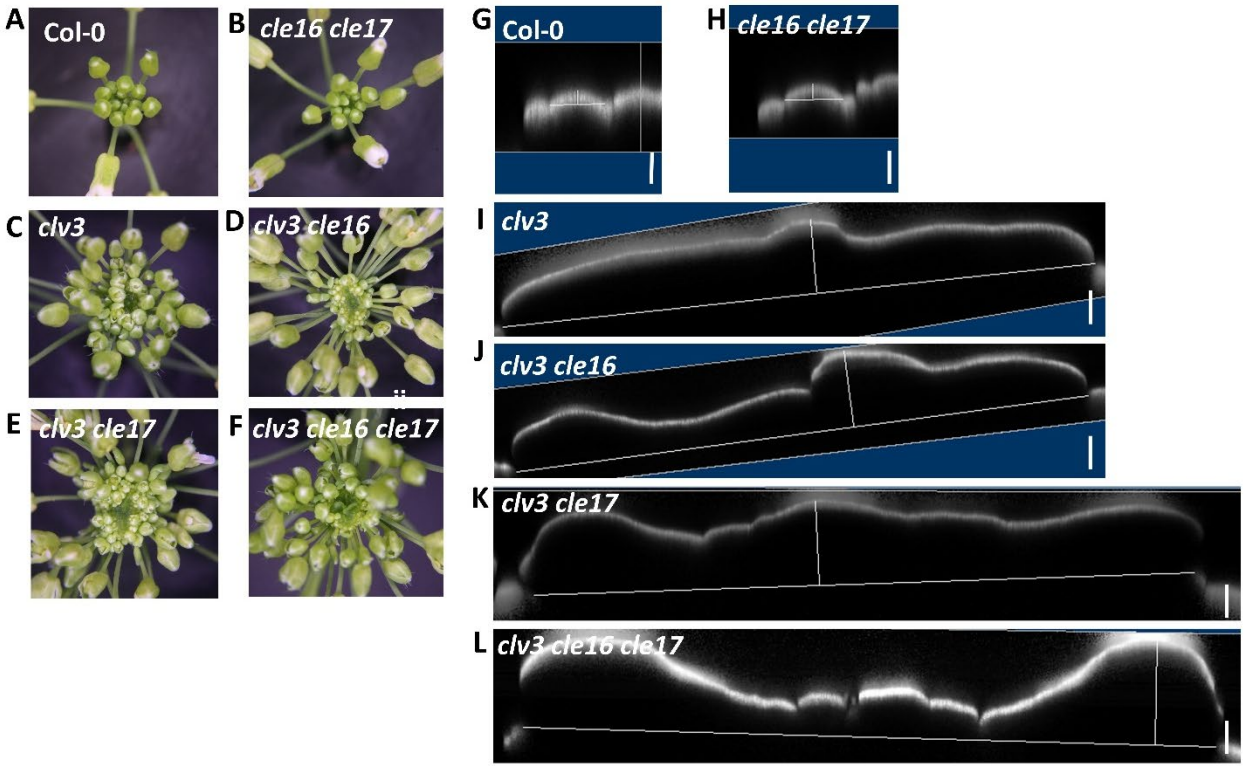

Fig. S4. *CLE16* and *CLE17* restrict stem cell accumulation in the inflorescence meristem in the absence of CLV3 activity, related to figure 2. Representative top-down view of inflorescences (A-F), and reconstructed longitudinal sections of inflorescence meristems from confocal stacks (G-L) from wild-type (A, G), *cle16 cle17* (B, H), *clv3* (C, I), *clv3 cle16* (D, J), *clv3 cle17* (E, K), and *clv3 cle16 cle17* (F, L) plants (n = 8 to 16). Scale bars: 300 µm.

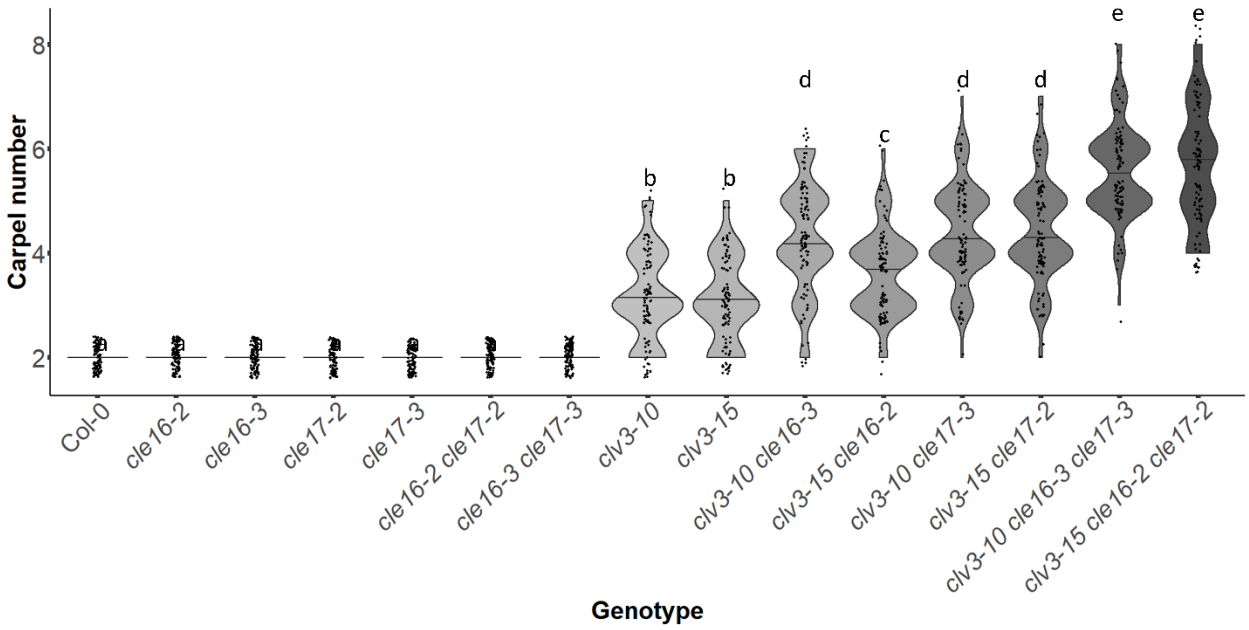

Fig. S5. Different combinations of *cle* alleles have the same effect on floral organ production, related to figure 3. Mean carpel number in wild-type, *cle16-2*, *cle16-3*, *cle17-2*, *cle17-3*, *cle16-2 cle17-2*, *cle16-3 cle17-3*, *clv3-10*, *clv3-15*, *clv3-10 cle16-3*, *clv3-15 cle16-2*, *clv3-10 cle17-3*, *clv3-15 cle17-2, clv3- 10 cle16-3 cle17-3* and *clv3-15 cle16-2 cle17-2* flowers (n = 100 flowers per genotype). Each dot in the violin plots represents the carpel number for an individual flower; and the middle line is the median. Statistical analysis was performed using one-way ANOVA and Tukey test; letters represent different significance groups at $P < 0.05$.

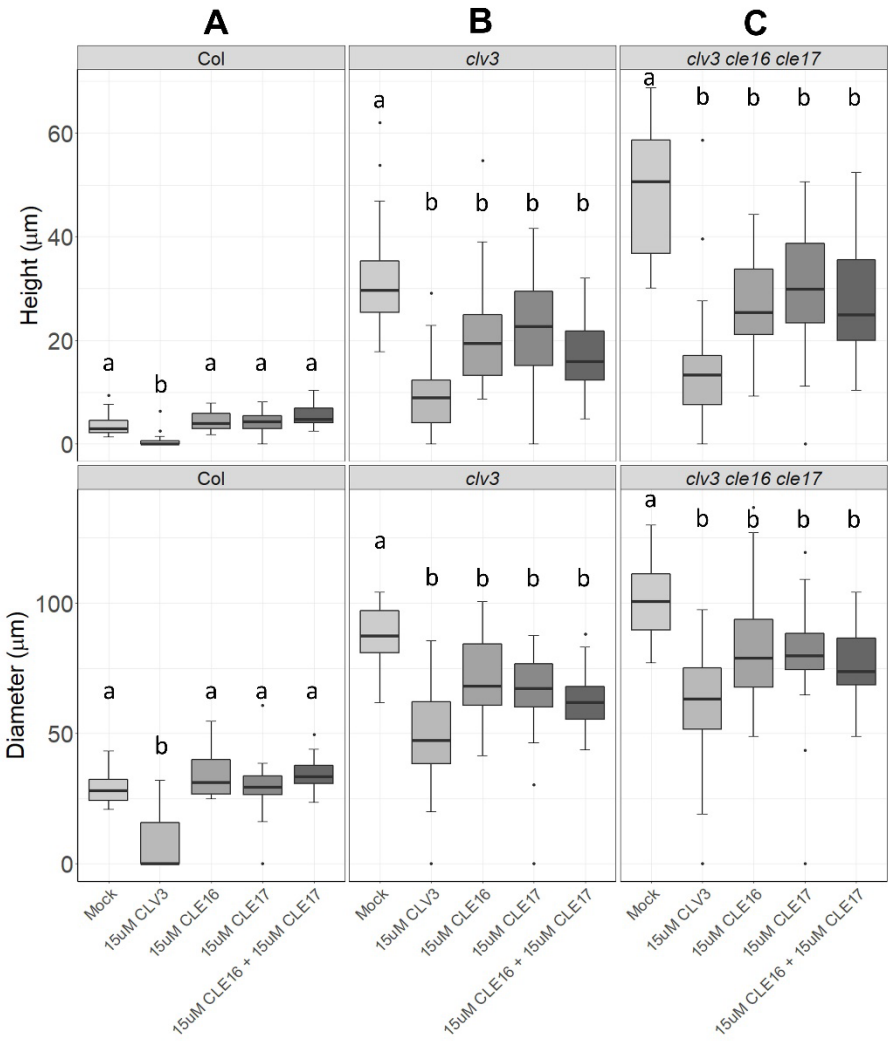

Fig. S6. CLE16 and CLE17 synthetic peptide treatments affect stem cell accumulation in the SAM in the absence of CLV3 activity, related to figure 4. Vegetative meristem size measurements of 7 DAG wild-type (A), *clv3* (B), and *clv3 cle16 cle17* (C) plants grown on MS plates containing a mock solution or 15 µM of synthetic CLV3, CLE16, CLE17, or CLE16 plus CLE17 peptide (n = 15 to 35). For the box plots, the bottom and top of the boxes represent the twenty-fifth and seventy-fifth percentile, respectively; the whiskers represent the minimum and maximum values; and the middle line is the median. Statistical analysis was performed using one-way ANOVA and Tukey test; letters represent different significance groups at $P < 0.05$.

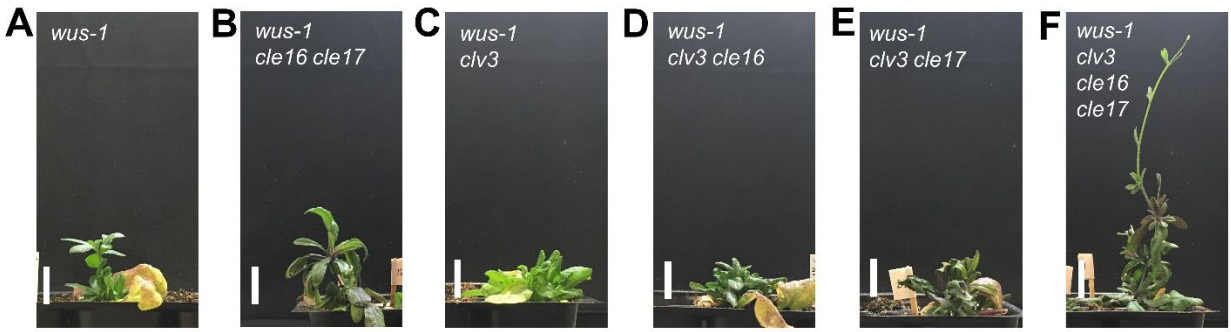

Fig. S7. Genetic interactions between *CLE16* and *CLE17* signaling pathways and *WUS*, related to figure 6. A-F, Side view of *wus-1* (A), *wus cle16 cle17* (B), *wus clv3* (C), *wus clv3 cle16* (D), *wus clv3 cle17* (E), and *wus clv3 cle16 cle17* (F) plants showing deficiency in shoot meristem maintenance. Scale bar: 2 cm.

Table S1. List of primers used in this study

Primer name	Sequence	Restriction enzyme
CLV3-F	ATGGATTCGAAGAGTTTTCTGCT	
CLV3-R	GACTCCCGAAATGGTAAAACCG	
CLE16-2-F	GAATCCAAAACCTGCTCTGC	MspI
CLE16-2-R	CGAAGGAGCAGTCAACACCT	
CLE17-2-F	ACTCCTCCGGAACAAGGTTT	BslI
CLE17-2-R	CTTCTGCACGCACTTTCTCA	